

Interstellar Medium (ISM)

Week 4

April 09 (Thursday), 2020

updated 04/06, 23:43

선광일 (Kwangil Seon)
KASI / UST

Neutral Medium 2

- Collisional Excitation & De-excitation
 - Intrinsic Line Profile
- Optical/UV Absorption Line
 - Curve of Growth

Collisional Excitation & De-excitation

- **Collisional Rate (Two Level Atom)**

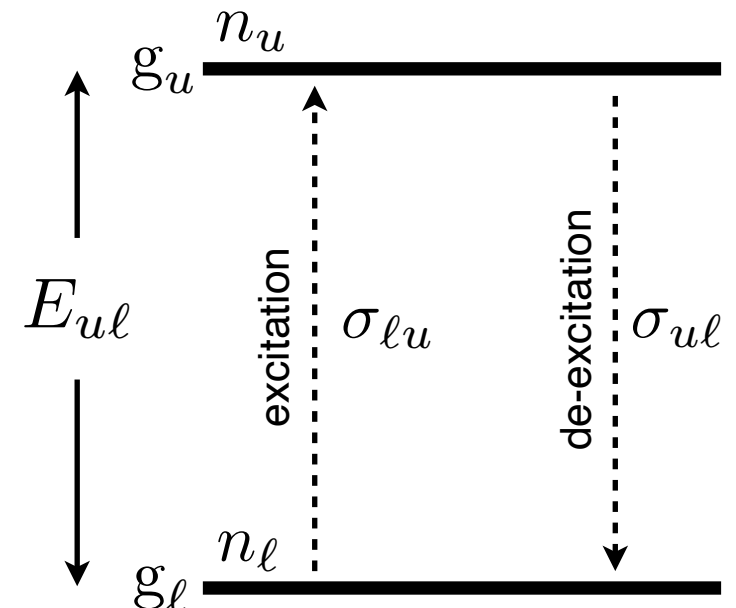
- ▶ The cross section $\sigma_{\ell u}$ for collisional excitation from a lower level ℓ to an upper level u is, in general, inversely proportional to the impact energy (or v^2) above the energy threshold E_{ul} and is zero below.
- ▶ The collisional cross section can be expressed in the following form using a dimensionless quantity called the ***collision strength*** $\Omega_{\ell u}$:

$$\begin{aligned}\sigma_{\ell u}(v) &= (\pi a_0^2) \left(\frac{hR_\infty}{\frac{1}{2}m_e v^2} \right) \frac{\Omega_{\ell u}}{g_\ell} \text{ cm}^2 \quad \text{for } \frac{1}{2}m_e v^2 > E_{ul} \\ &= \frac{h^2}{4\pi m_e^2 v^2} \frac{\Omega_{\ell u}}{g_\ell}\end{aligned}$$

or $\sigma_{\ell u}(E) = \frac{h^2}{8\pi m_e E} \frac{\Omega_{\ell u}}{g_\ell} \quad \left(E = \frac{1}{2}m_e v^2 \right)$

where, $a_0 = \frac{\hbar^2}{m_e e^2} = 5.12 \times 10^{13}$ cm, Bohr radius

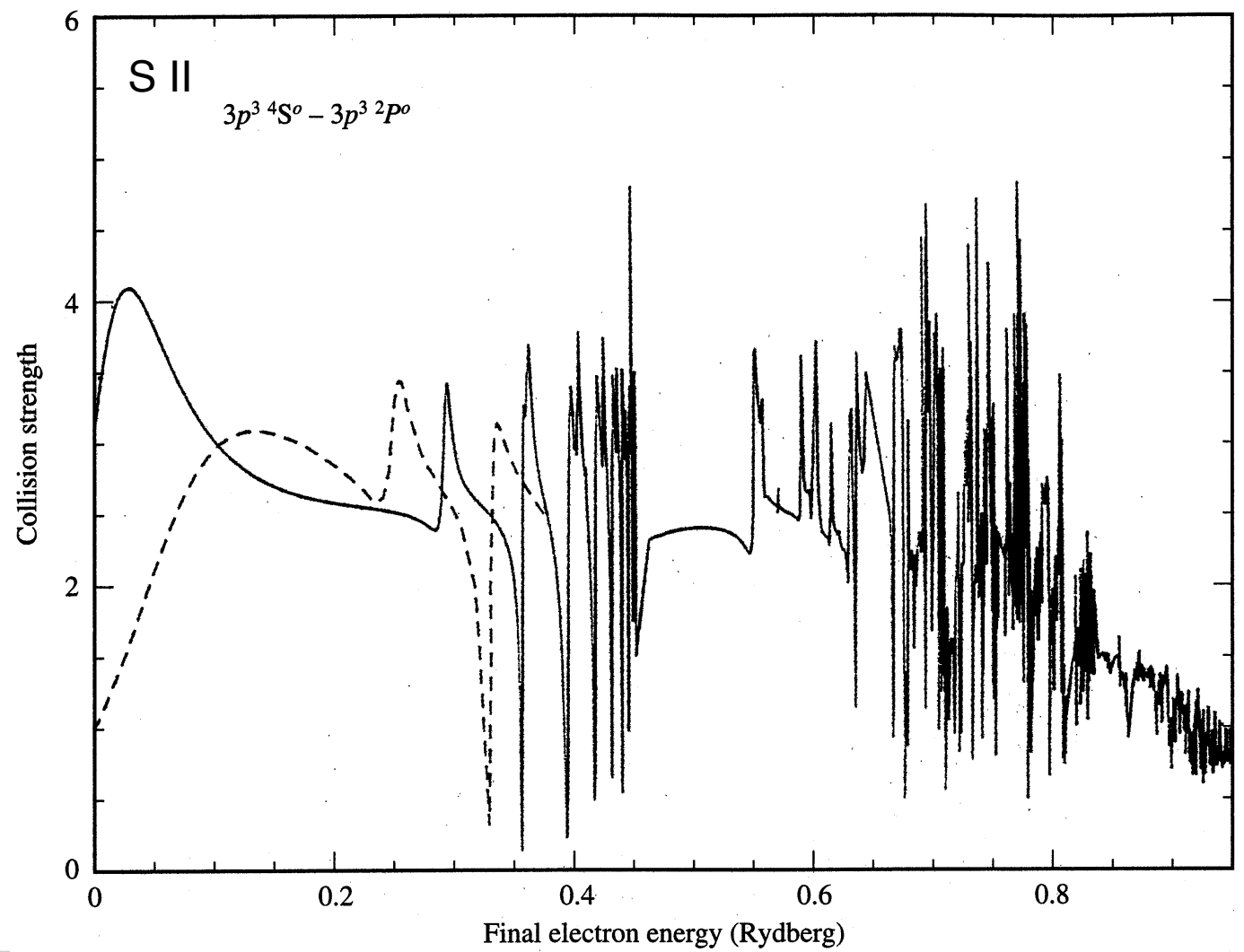
$$R_\infty = \frac{m_e e^4}{4\pi \hbar^3} = 109,737 \text{ cm}^{-1}, \text{ Rydberg constant} \quad \left(\hbar = \frac{h}{2\pi} \right)$$



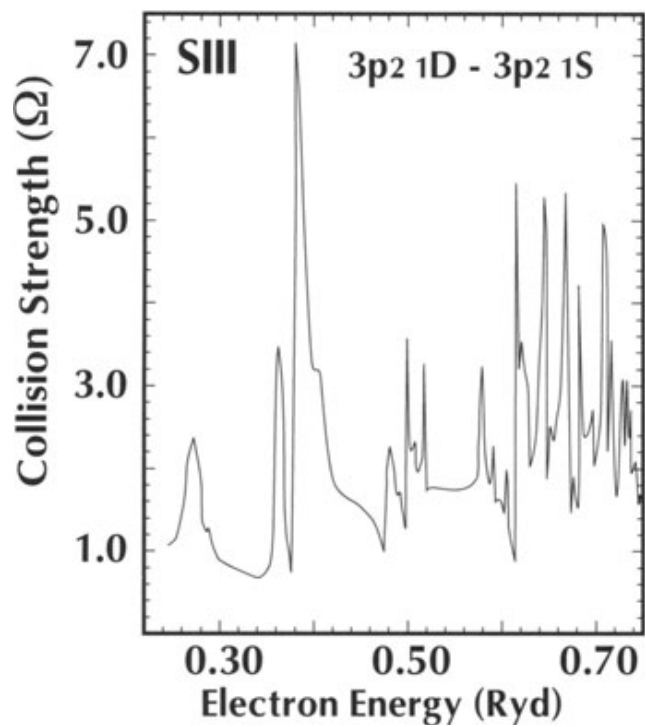
- ▶ The collision strength $\Omega_{\ell u}$ is a function of electron velocity (or energy) but is often approximately constant near the threshold. Here, g_ℓ and g_u are the statistical weights of the lower and upper levels, respectively.

- Collision Strength

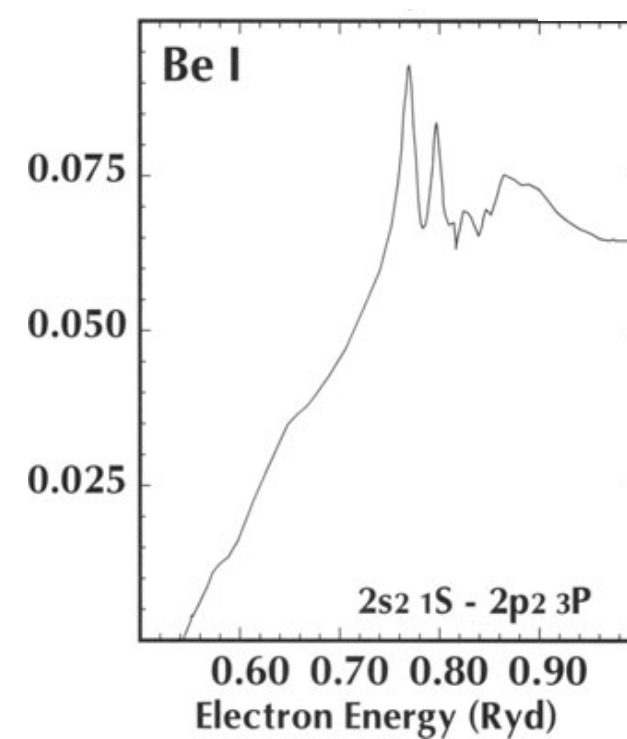
- Quantum mechanical calculations show that (1) the resonance structure in the collision strengths is important and (2) the collision strength increases with energy for neutral species.



Tayal (1996)



Badnell (1999)



solid - Ramsbottom et al. (1996)
dashed - Cai & Pradhan (1993)

- The averaged collision strength has a value in a range of

$$\langle \Omega_{ul} \rangle = \int_0^\infty \Omega_{ul}(E) e^{-E/k_B T} d(E/k_B T)$$

$$10^{-2} < \langle \Omega_{ul} \rangle < 10$$

- Advantage of using the collision strength is that (1) it removes the primary energy dependence for most atomic transitions and (2) they have the symmetry between the upper and the lower states.

The principle of detailed balance states that ***in thermodynamic equilibrium each microscopic process is balanced by its inverse.***

$$n_e n_\ell v_\ell \sigma_{\ell u}(v_\ell) f(v_\ell) dv_\ell = n_e n_u v_u \sigma_{u\ell}(v_u) f(v_u) dv_u$$

Here, v_ℓ and v_u are related by $\frac{1}{2}m_e v_\ell^2 = \frac{1}{2}m_e v_u^2 + E_{u\ell}$, and $f(v)$ is a Maxwell velocity distribution of electrons. Using the Boltzmann equation of thermodynamic equilibrium,

$$\frac{n_u}{n_\ell} = \frac{g_u}{g_\ell} \exp\left(-\frac{E_{u\ell}}{kT}\right)$$

we derive the following relation between the cross-sections for excitation and de-excitation are

$$g_\ell v_\ell^2 \sigma_{\ell u}(v_\ell) = g_u v_u^2 \sigma_{u\ell}(v_u) \quad \text{Here, } \frac{1}{2}m_e v_\ell^2 = \frac{1}{2}m_e v_u^2 + E_{u\ell}$$

or

$$g_\ell(E + E_{u\ell}) \sigma_{\ell u}(E + E_{u\ell}) = g_u E \sigma_{u\ell}(E)$$

and the symmetry of the collision strength between levels.

$$\Omega_{\ell u} = \Omega_{u\ell}$$

more precisely $\Omega_{u\ell}(E + E_{u\ell}) = \Omega_{u\ell}(E)$

These two relations were derived in the TE condition. However, ***the cross-sections are independent on the assumptions, and thus the above relations should be always satisfied.***

► Collisional excitation and de-excitation rates

The ***collisional de-excitation rate per unit volume per unit time, which is thermally averaged,*** is

$$\begin{aligned} \left(\frac{dn_\ell}{dt} \right)_{u \rightarrow \ell} &= n_e n_u \int_0^\infty v \sigma_{u\ell}(v) f(v) dv \\ &= n_e n_u k_{u\ell} \quad [\text{cm}^{-3} \text{ s}^{-1}] \end{aligned}$$

$$k_{u\ell} \equiv \langle \sigma v \rangle_{u \rightarrow \ell}$$

$$\begin{aligned} k_{u\ell} &= \int_0^\infty v \sigma_{u\ell}(v) f(v) dv \\ &= \left(\frac{2\pi\hbar^4}{k_B m_e^3} \right)^{1/2} T^{-1/2} \frac{\langle \Omega_{u\ell} \rangle}{g_u} \\ &= \frac{8.62942 \times 10^{-6}}{T^{1/2}} \frac{\langle \Omega_{u\ell} \rangle}{g_u} \quad [\text{cm}^3 \text{ s}^{-1}], \end{aligned}$$

$$\text{Here, } \langle \Omega_{u\ell} \rangle = \int_0^\infty \Omega_{u\ell}(E) e^{-E/k_B T} d(E/k_B T)$$

and the ***collisional excitation rate per unit volume per unit time*** is

$$\left(\frac{dn_u}{dt} \right)_{\ell \rightarrow u} = n_e n_\ell k_{\ell u}$$

$$k_{\ell u} \equiv \langle \sigma v \rangle_{\ell \rightarrow u}$$

$$\begin{aligned} k_{\ell u} &= \int_{v_{\min}}^\infty v \sigma_{\ell u}(v) f(v) dv \quad \text{Here, } \frac{1}{2} m_e v_{\min}^2 = E_{u\ell} \\ &= \left(\frac{2\pi\hbar^4}{k_B m_e^3} \right)^{1/2} T^{-1/2} \frac{\langle \Omega_{u\ell} \rangle}{g_\ell} \exp\left(-\frac{E_{u\ell}}{kT}\right) \end{aligned}$$

Here, $k_{\ell u}$ and $k_{u\ell}$ are the collisional rate coefficient for excitation and de-excitation coefficients in units of $\text{cm}^3 \text{ s}^{-1}$, respectively. We also note that ***the rate coefficients for collisional excitation and de-excitation are related by***

$$k_{\ell u} = \frac{g_u}{g_\ell} k_{u\ell} \exp\left(-\frac{E_{u\ell}}{kT}\right)$$

$$\langle \sigma v \rangle_{\ell \rightarrow u} = \frac{g_u}{g_\ell} \langle \sigma v \rangle_{u \rightarrow \ell} \exp\left(-\frac{E_{u\ell}}{kT}\right)$$

Sum rule for collision strengths

- Quantum mechanical sum rule for collision strengths for the case where one term consists of a singlet ($S = 0$ or $L = 0$) and the second consists of a multiplet: the collision strength of each fine structure level J is related to the total collision strength of the multiplet by

$$\Omega_{(SLJ, S'L'J')} = \frac{(2J' + 1)}{(2S' + 1)(2L' + 1)} \Omega_{(SL, S'L')}$$

Here, $(2J'+1)$ is the statistical weight of an individual level in the multiplet, and $(2S'+1)$ ($2L'+1$) is the statistical weight of the multiplet.

We can regard the collision strength as “shared” amongst these levels in proportion to the statistical weights of the individual levels ($g_J = 2J+1$).

- We will learn that ***the flux ratio between the fine structure lines in a multiplet is proportional to the ratio of their collision strengths, provided that the energy gap between the fine structure levels are small.*** Then, the flux ratio is determined by the ratio of their statistical weights.

- C-like ions ($1s^2 2s^2 2p^2 \rightarrow 1s^2 2s^2 2p^2$) forbidden or inter combination transitions.

ground states (triplet) - ${}^3P_0 : {}^3P_1 : {}^3P_2 = 1 : 3 : 5$

excited states (singlets) - ${}^1D_2, {}^1S_1$

- Li-like ions ($1s^2 2s^1 \rightarrow 1s^2 2p^1$) resonance transitions

ground state (singlet) - ${}^2S_{1/2}$

excited states (doublet) - ${}^2P_{3/2} : {}^2P_{1/2} = 2 : 1$

Collisionally-Excited Emission Line

- Emission line flux

- In the low density limit, the collisional rate between atoms and electrons is much slower than the (spontaneous) radiative de-excitation rate of the excited level. Thus, we can balance the collisional feeding into level u by the rate of radiative transition back down to level ℓ . The level population is determined by

$$n_e n_\ell k_{\ell u} = A_{u\ell} n_u$$

$$\frac{n_u}{n_\ell} = \frac{n_e k_{\ell u}}{A_{u\ell}}$$

$$= \frac{n_e}{A_{u\ell}} \beta \frac{\langle \Omega_{u\ell} \rangle}{g_\ell} T^{-1/2} \exp\left(-\frac{E_{u\ell}}{kT}\right)$$

where $A_{u\ell}$ is the Einstein coefficient for spontaneous emission. The line emissivity is given by

$$4\pi j_{u\ell} = E_{u\ell} A_{u\ell} n_u = E_{u\ell} n_e n_\ell k_{\ell u}$$

$$= n_e n_\ell E_{u\ell} \frac{8.62942 \times 10^{-6}}{T^{1/2}} \frac{\langle \Omega_{u\ell} \rangle}{g_\ell} \exp\left(-\frac{E_{u\ell}}{kT}\right) \text{ [erg cm}^{-3} \text{ s}^{-1}\text{]}$$

$$\simeq \beta \chi n_e^2 E_{u\ell} T^{-1/2} \frac{\langle \Omega_{u\ell} \rangle}{g_\ell} \exp\left(-\frac{E_{u\ell}}{kT}\right)$$

Here, $\beta = \left(\frac{2\pi\hbar^4}{km_e^2}\right)^{1/2} = 8.62942 \times 10^{-6}$
 $\chi = n_\ell/n_e$

For low temperature, the exponential term dominates because few electrons have energy above the threshold for collisional excitation, so that the line rapidly fades with decreasing temperature.

At high temperature, the $T^{-1/2}$ term controls the cooling rate, so the line fades slowly with increasing temperature.

-
- ▶ In **high-density limit**, the level population are set by the Boltzmann equilibrium, and the line emissivity is

$$\begin{aligned} \frac{n_u}{n_\ell} &= \frac{g_u}{g_\ell} \exp\left(-\frac{E_{u\ell}}{kT}\right) \\ 4\pi j_{u\ell} &= E_{\ell u} A_{u\ell} n_u \\ &= n_\ell E_{\ell u} A_{u\ell} \frac{g_u}{g_\ell} \exp\left(-\frac{E_{\ell u}}{kT}\right) \\ &\simeq \chi n_e E_{\ell u} A_{u\ell} \frac{g_u}{g_\ell} \exp\left(-\frac{E_{\ell u}}{kT}\right) \end{aligned}$$

Here, the line flux scales as n_e rather than n_e^2 , but the line flux tends to a constant value at high temperature.

- ▶ **Critical density** is defined as the density where the radiative depopulation rate matches the collisional de-excitation for the excited state.

$$\begin{aligned} A_{u\ell} n_u &= n_e n_u k_{u\ell} & \rightarrow n_{\text{crit}} &= A_{u\ell} \frac{g_u}{\beta \langle \Omega_{u\ell} \rangle} T^{1/2} \\ n_{\text{crit}} &= \frac{A_{u\ell}}{k_{u\ell}} & &= 1.2 \times 10^3 \frac{A_{u\ell}}{10^{-4} \text{ s}^{-1}} \frac{g_u}{\langle \Omega_{u\ell} \rangle} \left(\frac{T}{10^4 \text{ K}} \right)^{1/2} [\text{cm}^{-3}] \end{aligned}$$

- ▶ At densities higher than the critical density, collisional de-excitation becomes significant, and the forbidden lines will be weaker as the density increases.

At around the critical density, the “line emissivity vs density” plotted in log-log scale changes slope from +2 to +1.

- As can be seen in Tables and the formula, collisional de-excitation is negligible for resonance and most forbidden lines in the ISM.

| Ion | ℓ | u | | | $n_{\text{H,crit}}(u)$ | |
|-------|----------------------|----------------------|-------------------|----------------|--|---|
| | | | E_ℓ/k (K) | E_u/k (K) | $\lambda_{u\ell}$ (μm) | $T = 100 \text{ K}$ (cm^{-3}) |
| C II | $^2\text{P}_{1/2}^o$ | $^2\text{P}_{3/2}^o$ | 0 | 91.21 | 157.74 | 2.0×10^3 |
| CI | $^3\text{P}_0$ | $^3\text{P}_1$ | 0 | 23.60 | 609.7 | 620 |
| | $^3\text{P}_1$ | $^3\text{P}_2$ | 23.60 | 62.44 | 370.37 | 720 |
| O I | $^3\text{P}_2$ | $^3\text{P}_1$ | 0 | 227.71 | 63.185 | 2.5×10^5 |
| | $^3\text{P}_1$ | $^3\text{P}_0$ | 227.71 | 326.57 | 145.53 | 2.3×10^4 |
| Si II | $^2\text{P}_{1/2}^o$ | $^2\text{P}_{3/2}^o$ | 0 | 413.28 | 34.814 | 1.0×10^5 |
| Si I | $^3\text{P}_0$ | $^3\text{P}_1$ | 0 | 110.95 | 129.68 | 4.8×10^4 |
| | $^3\text{P}_1$ | $^3\text{P}_2$ | 110.95 | 321.07 | 68.473 | 9.9×10^4 |
| | | | | | | 3.5×10^4 |

Table 17.1 in [Draine]

- However, it is not true for the 21 cm hyperfine structure line of hydrogen.

- The critical density for 21cm line is

$$n_{\text{crit}} \sim 10^{-3} (T/100 \text{ K})^{-1/2} [\text{cm}^{-3}]$$

$$A_{u\ell} = 2.88 \times 10^{-15} [\text{s}^{-1}]$$

- The levels are thus essentially in collisional equilibrium in the CNM.

Collision strengths at $T = 10^4 \text{ K}$

Table 4.1 in The Interstellar Medium [Lequeux]

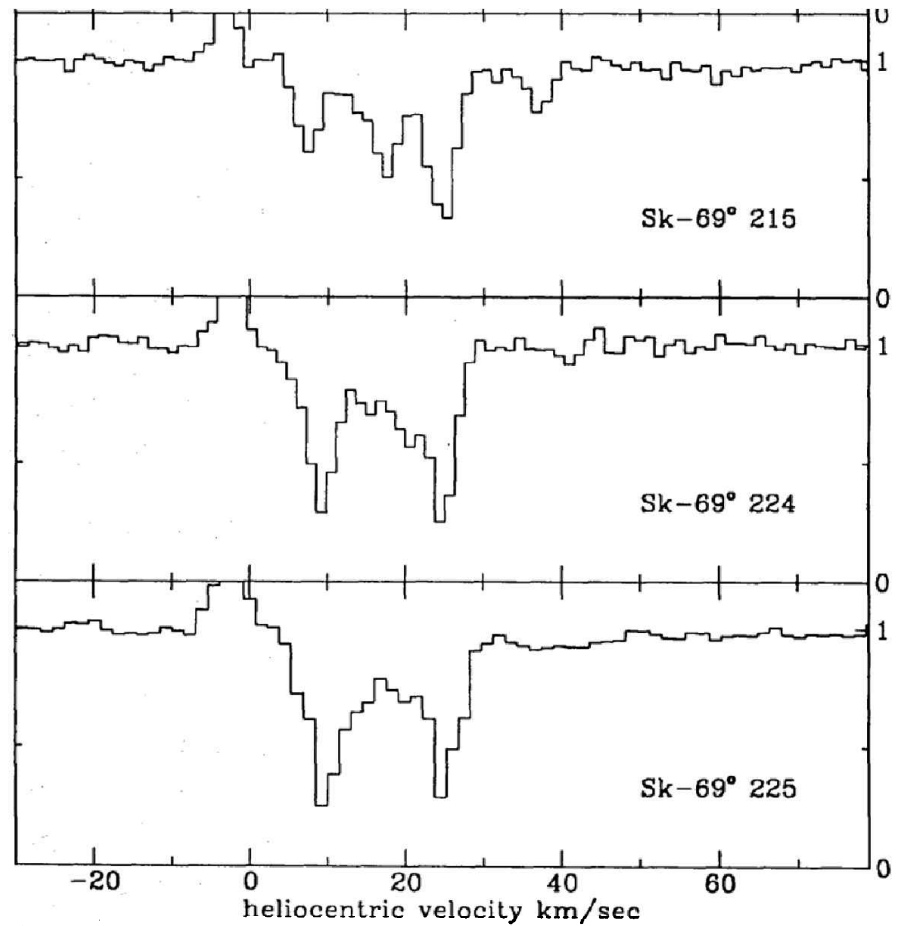
| Ion | Transition l-u | λ μm | A_{ul} s^{-1} | Ω_{ul} | n_{crit} cm^{-3} |
|--------|---------------------------------------|----------------------------|-----------------------------|---------------|---------------------------------------|
| C I | $^3\text{P}_0 - ^3\text{P}_1$ | 609.1354 | 7.93×10^{-8} | - | (500) |
| | $^3\text{P}_1 - ^3\text{P}_2$ | 370.4151 | 2.65×10^{-7} | - | (3000) |
| C II | $^2\text{P}_{1/2} - ^2\text{P}_{3/2}$ | 157.741 | 2.4×10^{-6} | 1.80 | 47 (3000) |
| N II | $^3\text{P}_0 - ^3\text{P}_1$ | 205.3 | 2.07×10^{-6} | 0.41 | 41 |
| | $^3\text{P}_1 - ^3\text{P}_2$ | 121.889 | 7.46×10^{-6} | 1.38 | 256 |
| | $^3\text{P}_2 - ^1\text{D}_2$ | 0.65834 | 2.73×10^{-3} | 2.99 | 7700 |
| | $^3\text{P}_1 - ^1\text{D}_2$ | 0.65481 | 9.20×10^{-4} | 2.99 | 7700 |
| N III | $^2\text{P}_{1/2} - ^2\text{P}_{3/2}$ | 57.317 | 4.8×10^{-5} | 1.2 | 1880 |
| O I | $^3\text{P}_2 - ^3\text{P}_1$ | 63.184 | 8.95×10^{-5} | - | $2.3 \times 10^4 (5 \times 10^5)$ |
| | $^3\text{P}_1 - ^3\text{P}_0$ | 145.525 | 1.7×10^{-5} | - | $3400 (1 \times 10^5)$ |
| | $^3\text{P}_2 - ^1\text{D}_2$ | 0.63003 | 6.3×10^{-3} | - | 1.8×10^6 |
| O II | $^4\text{S}_{3/2} - ^2\text{D}_{5/2}$ | 0.37288 | 3.6×10^{-5} | 0.88 | 1160 |
| | $^4\text{S}_{3/2} - ^2\text{D}_{3/2}$ | 0.37260 | 1.8×10^{-4} | 0.59 | 3890 |
| O III | $^3\text{P}_0 - ^3\text{P}_1$ | 88.356 | 2.62×10^{-5} | 0.39 | 461 |
| | $^3\text{P}_1 - ^3\text{P}_2$ | 51.815 | 9.76×10^{-5} | 0.95 | 3250 |
| | $^3\text{P}_2 - ^1\text{D}_2$ | 0.50069 | 1.81×10^{-2} | 2.50 | 6.4×10^5 |
| | $^3\text{P}_1 - ^1\text{D}_2$ | 0.49589 | 6.21×10^{-3} | 2.50 | 6.4×10^5 |
| | $^1\text{D}_2 - ^1\text{S}_0$ | 0.43632 | 1.70 | 0.40 | 2.4×10^7 |
| Ne II | $^2\text{P}_{1/2} - ^2\text{P}_{3/2}$ | 12.8136 | 8.6×10^{-3} | 0.37 | 5.9×10^5 |
| Ne III | $^3\text{P}_2 - ^3\text{P}_1$ | 15.5551 | 3.1×10^{-2} | 0.60 | 1.27×10^5 |
| | $^3\text{P}_1 - ^3\text{P}_0$ | 36.0135 | 5.2×10^{-3} | 0.21 | 1.82×10^4 |
| Si II | $^2\text{P}_{1/2} - ^2\text{P}_{3/2}$ | 34.8152 | 2.17×10^{-4} | 7.7 | (3.4×10^5) |
| S II | $^4\text{S}_{3/2} - ^2\text{D}_{5/2}$ | 0.67164 | 2.60×10^{-4} | 4.7 | 1240 |
| | $^4\text{S}_{3/2} - ^2\text{D}_{3/2}$ | 0.67308 | 8.82×10^{-4} | 3.1 | 3270 |
| S III | $^3\text{P}_0 - ^3\text{P}_1$ | 33.4810 | 4.72×10^{-4} | 4.0 | 1780 |
| | $^3\text{P}_1 - ^3\text{P}_2$ | 18.7130 | 2.07×10^{-3} | 7.9 | 1.4×10^4 |
| S IV | $^2\text{P}_{1/2} - ^2\text{P}_{3/2}$ | 10.5105 | 7.1×10^{-3} | 8.5 | 5.0×10^4 |
| Ar II | $^2\text{P}_{1/2} - ^2\text{P}_{3/2}$ | 6.9853 | 5.3×10^{-2} | 2.9 | 1.72×10^6 |
| Ar III | $^3\text{P}_2 - ^3\text{P}_1$ | 8.9914 | 3.08×10^{-2} | 3.1 | 2.75×10^5 |
| | $^3\text{P}_1 - ^3\text{P}_0$ | 21.8293 | 5.17×10^{-3} | 1.3 | 3.0×10^4 |
| Fe II | $^6\text{D}_{7/2} - ^6\text{D}_{5/2}$ | 35.3491 | 1.57×10^{-3} | - | (3.3×10^6) |
| | $^6\text{D}_{9/2} - ^6\text{D}_{7/2}$ | 25.9882 | 2.13×10^{-3} | - | (2.2×10^6) |

Overall Properties of the CNM

- Overall properties of the CNM
 - Temperature $T \sim 100 \text{ K}$
 - Mean kinetic energy per particle $\langle E \rangle = (3/2)kT \sim 0.013 \text{ eV}$
 - Number density
 - ▶ $n_{\text{atom}} \sim 30 \text{ cm}^{-3}$ for atoms
 - ▶ $n_e \sim 0.04 \text{ cm}^{-3}$ for free electrons
 - Thermal velocity
 - ▶ $v_{\text{th}}(\text{H}) \sim 1.6 \text{ km s}^{-1}$ for hydrogen atoms
 - ▶ $v_{\text{th}}(e) \sim 67 \text{ km s}^{-1}$ for free electrons
 - Mean free path
 - ▶ $\lambda_{\text{mfp}}(\text{HH}) \sim 0.74 \text{ AU}$ for atom-atom collisions
 - ▶ $\lambda_{\text{mfp}}(e\text{H}) \sim 1700 \text{ AU}$ for atom-electron collisions
 - ▶ $\lambda_{\text{mfp}}(ee) \sim 1.9 \times 10^{-3} \text{ AU}$ for electron-electron collisions
 - Collisional time scale
 - ▶ $t_{\text{coll}}(\text{HH}) \sim 2.2 \text{ yr}$ for atom-atom collisions
 - ▶ $t_{\text{coll}}(e\text{H}) \sim 120 \text{ yr}$ for atom-electron collisions
 - ▶ $t_{\text{coll}}(ee) \sim 1.2 \text{ hr}$ for electron-electron collision

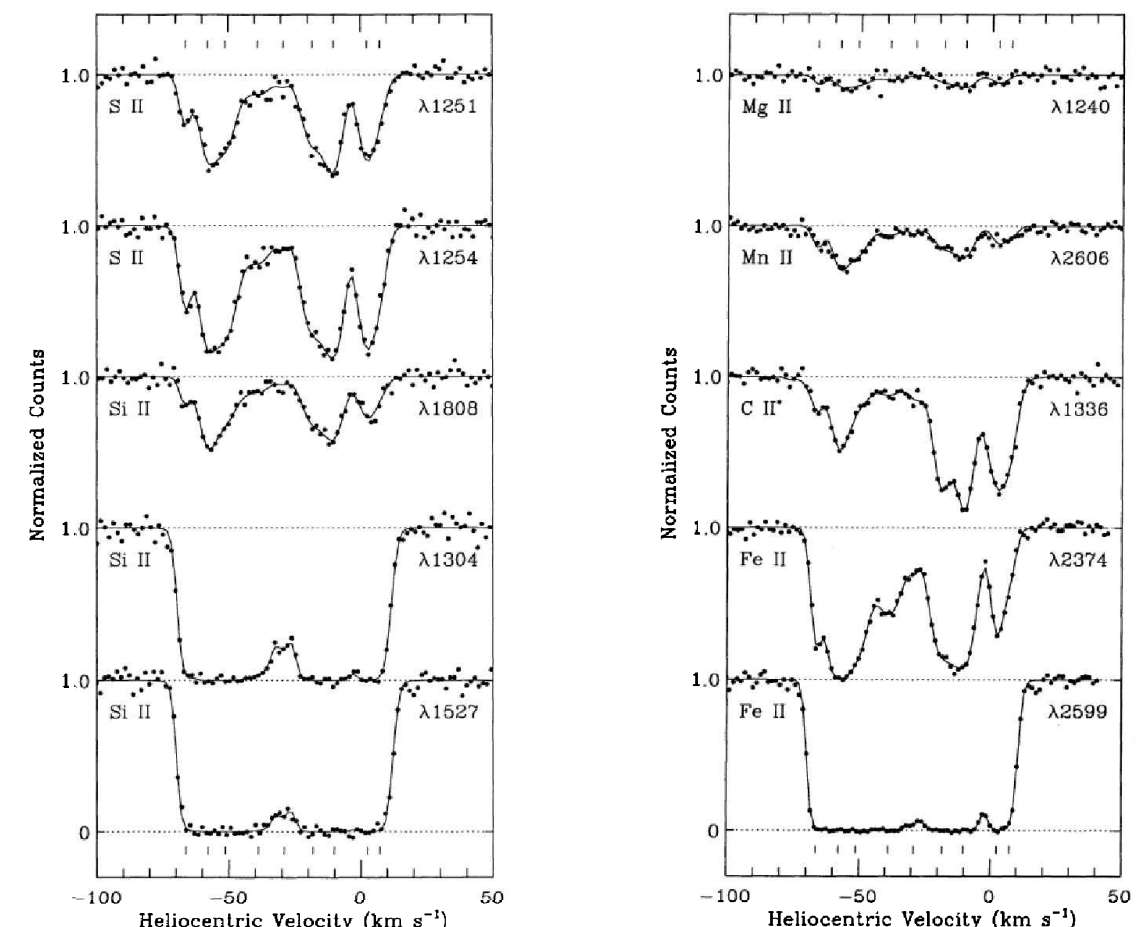
Observations of Absorption Lines Toward the CNM

- The CNM gives rise to a number of absorption features in the spectra of hot background stars.
 - The most prominent absorption lines at visible wavelengths are Ca II K and H lines at $\lambda = 3933, 3968 \text{ \AA}$, and Na I D₁ and D₂ doublet lines at $\lambda = 5890, 5896 \text{ \AA}$.



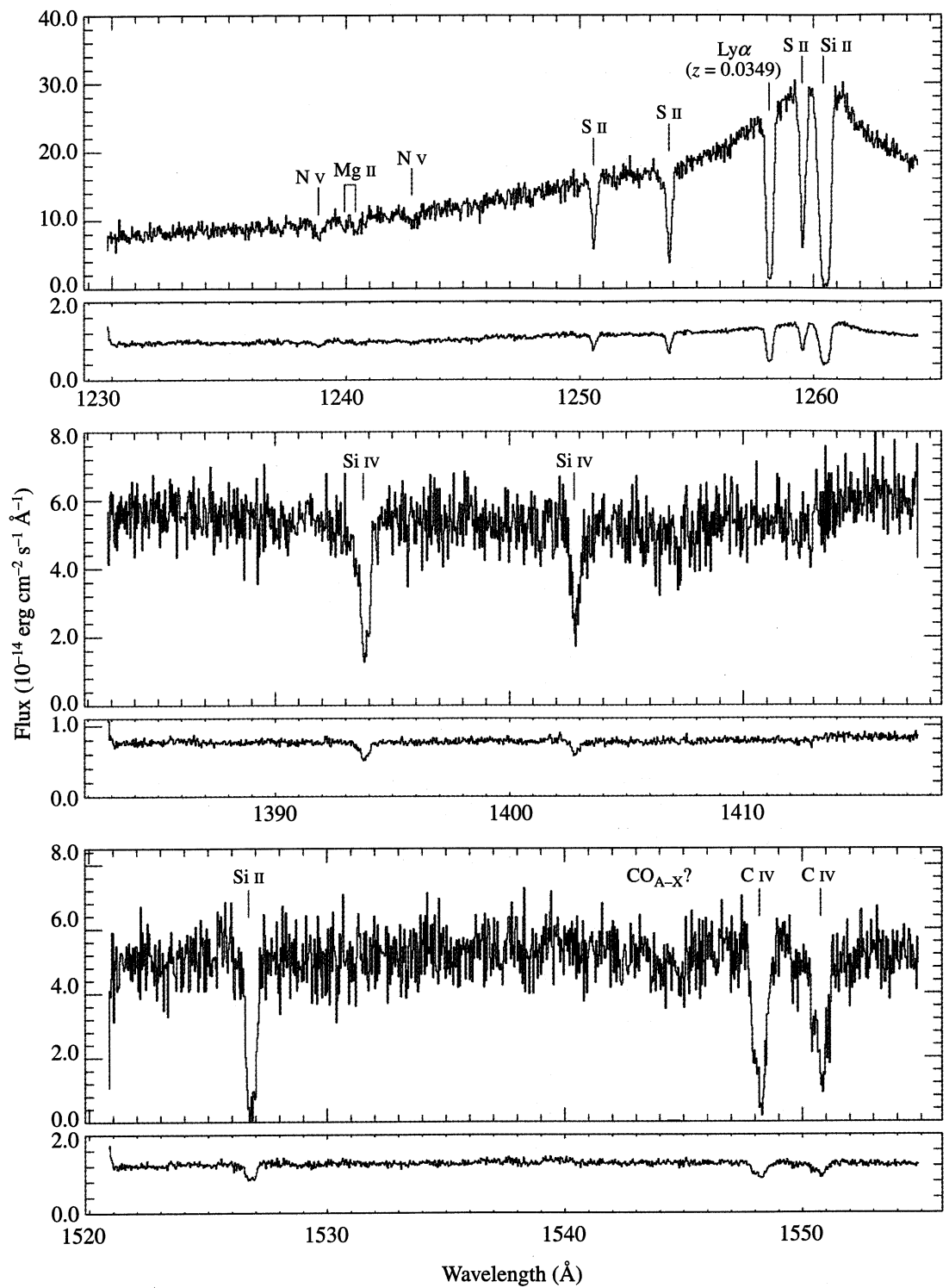
Na I D₂ interstellar absorption line seen along 3 lines of sight to stars in LMC (Molaro et al. 1993)

[Note] The cold gas is ~ 100 pc away from Earth, meaning that 5 arcmin corresponds to ~ 0.15 pc.



UV interstellar absorption lines toward an O-type star HD93521. (Spitzer & Fitzpatrick 1993)

[Note] (1) multiple velocity components and (2) line saturation on Si II and Fe II.
The multiple velocities are due primarily to the differential rotation of our galaxy. (clouds at different distances)



Interstellar absorption lines toward the
Seyfert 1 galaxy ESO 141-055.

Figure 5.5 in Physics and Chemistry of the Interstellar
Medium [Kwok]

-
- The alkali metals (Li, K, and Na) and alkaline earth metals (Ca) produce absorption lines at visible wavelengths ($4000 \text{ \AA} < \lambda < 7300 \text{ \AA}$, $1.7 \text{ eV} < E < 3.1 \text{ eV}$); these elements have loosely bound outer electrons.
 - Most other elements produce UV absorption lines ($\lambda < 4000 \text{ \AA}$, $E > 3.1 \text{ eV}$).
 - Therefore, the study of the CNM was extensively made by the launch of orbiting UV telescopes (Copernicus, IUE, etc).
 - In particular, Ly α ($\lambda = 1215.67 \text{ \AA}$; $E = 10.2 \text{ eV}$) from hydrogen.
 - Interstellar absorption lines at visible wavelengths were also found from neutral atoms such as Ca I, K I, Li I, ions such as Ti II, and diatomic molecules such as CH, NH, CN, CH⁺ and C₂.
 - [Note] The first discovery of interstellar molecules was made by the detection of CH absorption at $\lambda \sim 4300$ (4315) \AA (Swings & Rosenfeld 1937), not at radio wavelengths.
 - CH, NH, and CN are referred to as “radicals”, in chemistry, meaning molecules that contain at least one unpaired electron. They quickly combine with one another, or with single atoms in laboratory. But, in the low density of the ISM, they have long lifetimes.

-
- The composition and excitation of interstellar gas can be studied using absorption lines that appear in the spectra of background stars (or other sources).
 - The interstellar lines are typically narrow compared to spectral features produced by absorption in stellar photospheres, and in practice can be readily distinguished.
 - For instance, consider the Fraunhofer lines in the Sun's spectrum. The Ca H and K lines, with equivalent widths of 14\AA and 19\AA respectively, are the strongest absorption lines. The Na I D₁ and D₂ lines have equivalent widths of 0.6\AA and 0.8\AA .
 - However, for many interstellar lines, the equivalent width is sufficiently small that the m\AA is a convenient unit.
 - It is normally possible to detect absorption only by the ground state (and perhaps the excited fine-structure levels of the ground electronic state) - the populations in the excited electronic states are too small to be detected in absorption.
 - The widths of absorption lines are usually determined by Doppler broadening, with line widths of a few km s⁻¹ (or $\Delta\lambda/\lambda \approx 10^{-5}$) - often observed in cool clouds.
 - Absorption lines (and emission lines) contains a lots of information about number density, temperature, chemical abundances, ionization states, and excitation states.
 - However, interpreting the information requires understanding the ways in which light interacts with baryonic matter, radiative transfer.
 - **We need to know the line profile to analyze absorption lines.**

Line Profile: Classical model

- **Lorentz Oscillator Model** to describe the interaction between atoms and electric fields
 - The electron (with a small mass) is bound to the nucleus of the atom (with a much larger mass) by a force that behaves according to Hooke's Law (a spring-like force).
 - An applied electric field would then interact with the charge of the electron, causing “stretching” or “compression” of the spring.
 - ***The electron's equation of motion:***

$$m\ddot{\mathbf{x}} = -k\mathbf{x} + \mathbf{F}_{\text{ext}} + \mathbf{F}_{\text{rad}}$$

$k = m\omega_0^2$, where k = spring constant

ω_0 = natural (fundamental or resonant) frequency

\mathbf{F}_{ext} = external force, driving force, or external electric field

\mathbf{F}_{rad} = radiation reaction force (radiation damping)
the damping of a charge's motion which arises because of
the emission of radiation

[1] Spontaneous Emission : Damping, Free Oscillator

- **Undriven Harmonically Bound Particles** (free oscillator)
 - Since an oscillating electron represents a continuously accelerating charge, the electron will radiate energy.
 - The energy radiated away must come from the particle's own energy (energy conservation). In other words, **there must be a force acting on a particle by virtue of the radiation it produces. This is called the *radiation reaction force*.**
 - Let's derive the formula for the radiation reaction force from the fact that the energy radiated must be compensated for by the work done against the radiation reaction force.
 - On one hand, the radiative loss rate of energy, averaged over one cycle of the oscillating dipole, can be represented by the radiative reaction force:

$$\frac{dW}{dt} = \langle \mathbf{F}_{\text{rad}} \cdot \dot{\mathbf{x}} \rangle$$

- On the other hand, from the Larmor's formula for a dipole, the radiative loss will be:

$$\frac{dW}{dt} = -\frac{2e^2 \langle |\ddot{\mathbf{x}}|^2 \rangle}{3c^3}$$

[1] Spontaneous Emission : Abraham-Lorentz formula

$$\therefore \langle \mathbf{F}_{\text{rad}} \cdot \dot{\mathbf{x}} \rangle = -\frac{2e^2 \langle |\ddot{\mathbf{x}}|^2 \rangle}{3c^3}$$

Here, $\langle |\ddot{\mathbf{x}}|^2 \rangle \equiv \frac{1}{\tau} \int_{-\tau/2}^{\tau/2} \ddot{\mathbf{x}} \cdot \ddot{\mathbf{x}} dt$ where τ is the oscillation period.

$$= \frac{1}{\tau} \ddot{\mathbf{x}} \cdot \dot{\mathbf{x}} \Big|_{-\tau/2}^{\tau/2} - \frac{1}{\tau} \int_{-\tau/2}^{\tau/2} \ddot{\mathbf{x}} \cdot \dot{\mathbf{x}} dt$$

We assume that the initial and final states are the same: $\ddot{\mathbf{x}} \cdot \dot{\mathbf{x}}(-\tau/2) = \ddot{\mathbf{x}} \cdot \dot{\mathbf{x}}(\tau/2)$

Then,

$$\langle |\ddot{\mathbf{x}}|^2 \rangle = -\frac{1}{\tau} \int_{-\tau/2}^{\tau/2} \ddot{\mathbf{x}} \cdot \ddot{\mathbf{x}} dt = -\langle \ddot{\mathbf{x}} \cdot \dot{\mathbf{x}} \rangle \rightarrow \langle \mathbf{F}_{\text{rad}} \cdot \dot{\mathbf{x}} \rangle = \frac{2e^2 \langle \ddot{\mathbf{x}} \cdot \dot{\mathbf{x}} \rangle}{3c^3}$$

Therefore, we can obtain

$$\mathbf{F}_{\text{rad}} = \frac{2e^2 \ddot{\mathbf{x}}}{3c^3} : \text{Abraham-Lorentz formula}$$

- **Abraham-Lorentz formula:**

$$\mathbf{F}_{\text{rad}} = \frac{2e^2 \ddot{\mathbf{x}}}{3c^3}$$

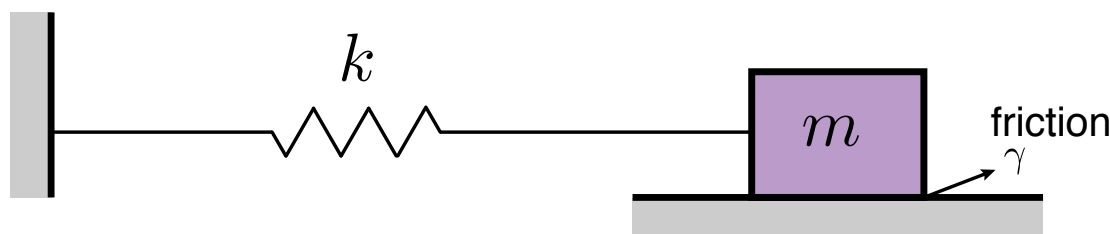
- This formula depends on the derivative of acceleration. This increases the degree of the equation of motion of a particle and can lead to some nonphysical behavior if not used properly and consistently.
- For a simple harmonic oscillator with a frequency ω_0 , we can avoid the difficulty by using

$$\ddot{\mathbf{x}} = -\omega_0^2 \dot{\mathbf{x}}$$

- ***This is a good assumption as long as the energy is to be radiated on a time scale that is long compared to the period of oscillation ($\gamma \ll \omega_0$)***. In this regime, ***radiation reaction may be considered as a perturbation on the particle's motion***.

We then rewrite the radiation reaction force as

$$\mathbf{F}_{\text{rad}} = -\frac{2e^2 \omega_0^2}{3c^3} \dot{\mathbf{x}} = -m\gamma \dot{\mathbf{x}}, \quad \gamma \equiv \frac{2e^2 \omega_0^2}{3mc^3} : \text{ damping constant}$$



$$m\ddot{\mathbf{x}} + k\mathbf{x} + m\gamma \dot{\mathbf{x}} = 0$$

This is the equation for a string-mass system subject to friction damping.

- Therefore, the equation of motion of the electron in a Lorentz atom is

$$\ddot{\mathbf{x}} + \gamma \dot{\mathbf{x}} + \omega_0^2 \mathbf{x} = 0$$

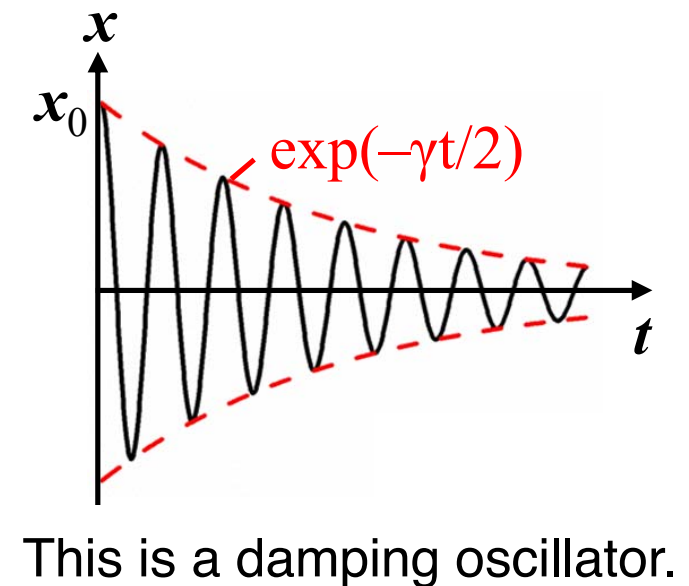
- This equation may be solved by assuming that $x(t) \propto e^{\alpha t}$.

$$\begin{aligned}\alpha^2 + \gamma\alpha + \omega_0^2 &= 0 \rightarrow \alpha = -(\gamma/2) \pm \sqrt{(\gamma/2)^2 - \omega_0^2} \\ &= -\gamma/2 \pm i\omega_0 + \mathcal{O}(\gamma^2/\omega_0^2)\end{aligned}$$

Here, we assumed $\gamma \ll \omega_0$.

- Assuming initial conditions: $x(0) = x_0$, $\dot{x}(0) = 0$ at $t = 0$
- we have

$$x(t) = \frac{1}{2}x_0 \left[e^{-(\gamma/2 - i\omega_0)t} + e^{-(\gamma/2 + i\omega_0)t} \right] = x_0 e^{-\gamma t/2} \cos \omega_0 t \quad \longrightarrow$$



- Power spectrum:

$$\bar{x}(\omega) = \frac{1}{2\pi} \int_0^\infty x(t) e^{i\omega t} dt = \frac{x_0}{4\pi} \left[\frac{1}{\gamma/2 - i(\omega + \omega_0)} + \frac{1}{\gamma/2 - i(\omega - \omega_0)} \right]$$

- This becomes large in the vicinity of $\omega = \omega_0$ and $\omega = -\omega_0$.
- We are ultimately interested only in positive frequencies, and only in regions in which the values become large. Therefore, we obtain

$$\bar{x}(\omega) \approx \frac{x_0}{4\pi} \frac{1}{\gamma/2 - i(\omega - \omega_0)}, \quad |\bar{x}(\omega)|^2 = \left(\frac{x_0}{4\pi} \right)^2 \frac{1}{(\omega - \omega_0)^2 + (\gamma/2)^2}$$

[1] Spontaneous Emission: Line profile

- Recall the Larmor's formula:

$$\frac{dW}{d\omega} = \frac{8\pi\omega^4}{3c^3} e^2 |\bar{x}(\omega)|^2$$

- Energy radiated per unit frequency:

$$\begin{aligned}\frac{dW}{d\omega} &= \frac{8\pi\omega^4}{3c^3} \frac{e^2 x_0^2}{(4\pi)^2} \frac{1}{(\omega - \omega_0)^2 + (\gamma/2)^2} = \frac{1}{2} m \left(\frac{\omega^4}{\omega_0^2} \right) x_0^2 \frac{\gamma/2\pi}{(\omega - \omega_0)^2 + (\gamma/2)^2} \\ &\approx \frac{1}{2} m \omega_0^2 x_0^2 \frac{\gamma/2\pi}{(\omega - \omega_0)^2 + (\gamma/2)^2}\end{aligned}$$

- For a harmonic oscillator, note that the equation of motion is $\mathbf{F} = -k\mathbf{x} = -m\omega_0^2\mathbf{x}$, spring constant is $k = m\omega_0^2$, and the potential energy (energy stored in spring) is $(1/2)kx_0^2$.

- From

$$\int_{-\infty}^{\infty} \frac{\gamma/2\pi}{(\omega - \omega_0)^2 + (\gamma/2)^2} d\omega = \frac{1}{\pi} \tan^{-1} \{ 2(\omega - \omega_0)/\gamma \} \Big|_{-\infty}^{\infty} = 1$$

- Note that the total emitted energy is equal to the initial potential energy of the oscillator:

$$W = \int_0^{\infty} \frac{dW}{d\omega} d\omega = \frac{1}{2} k \omega_0^2$$

- Profile of the emitted spectrum:

$$\phi(\omega) = \frac{\gamma/2\pi}{(\omega - \omega_0)^2 + (\gamma/2)^2}$$

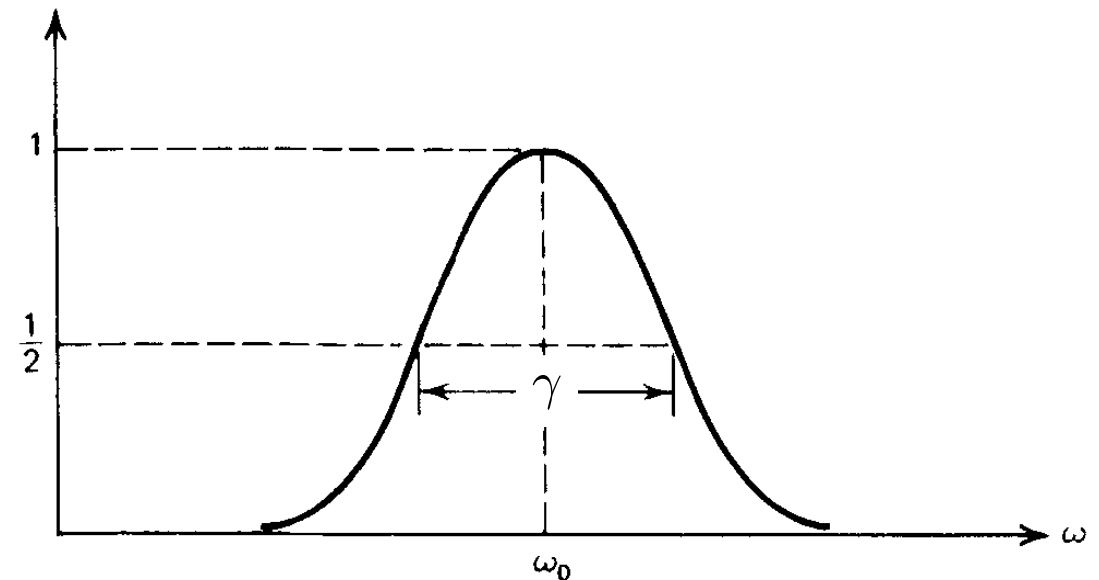
This is the Lorentz (natural) line profile.

- Damping constant is the full width at half maximum (FWHM).

$$\phi(\omega) = \frac{\gamma/2\pi}{(\omega - \omega_0)^2 + (\gamma/2)^2}$$

$$\phi(\nu) = \frac{\gamma/4\pi^2}{(\nu - \nu_0)^2 + (\gamma/4\pi)^2}$$

Note $\phi(\omega)d\omega = \phi(\nu)d\nu$



- The line width $\Delta\omega = \gamma$ is a universal constant when expressed in terms of wavelength:

$$\lambda = \frac{2\pi c}{\omega}$$

$$\begin{aligned} \Delta\lambda &= 2\pi c \frac{\Delta\omega}{\omega^2} = 2\pi c \frac{2}{3} \frac{r_e}{c} \quad \leftarrow \quad \left(\Delta\omega = \gamma = \frac{2}{3} r_e \frac{\omega_0^2}{c} \right) \\ &= \frac{4}{3} \pi r_e \\ &= 1.2 \times 10^{-4} \text{\AA} \end{aligned}$$

However, in Quantum Mechanics, the line width is not a universal constant.

[2] Absorption/Scattering : Driven Oscillator

- **Driven Harmonically Bound Particles** (forced oscillators)

- Electron's equation of motion (electric charge = $-e$): $\mathbf{F}_{\text{ext}} = -e\mathbf{E}_0 e^{i\omega t}$

$$\ddot{\mathbf{x}} + \gamma \dot{\mathbf{x}} + \omega_0^2 \mathbf{x} = -\frac{e\mathbf{E}_0}{m} e^{i\omega t}$$



- A particular solution for this inhomogeneous differential equation:

$$\mathbf{x} = \mathbf{x}_0 e^{i\omega t} \equiv |\mathbf{x}_0| e^{i(\omega t + \delta)} \rightarrow (-\omega^2 + i\omega\gamma + \omega_0^2) \mathbf{x}_0 e^{i\omega t} = -\frac{e\mathbf{E}_0}{m} e^{i\omega t}$$

$$\mathbf{x}_0 = \frac{(e/m)\mathbf{E}_0}{(\omega^2 - \omega_0^2) - i\omega\gamma}$$

$$\mathbf{x}_0 = |\mathbf{x}_0| e^{i\delta} \propto (\omega^2 - \omega_0^2) + i\omega\gamma \rightarrow \delta = \tan^{-1} \left(\frac{\omega\gamma}{\omega^2 - \omega_0^2} \right)$$

The response is slightly out of phase with respect to the imposed field.

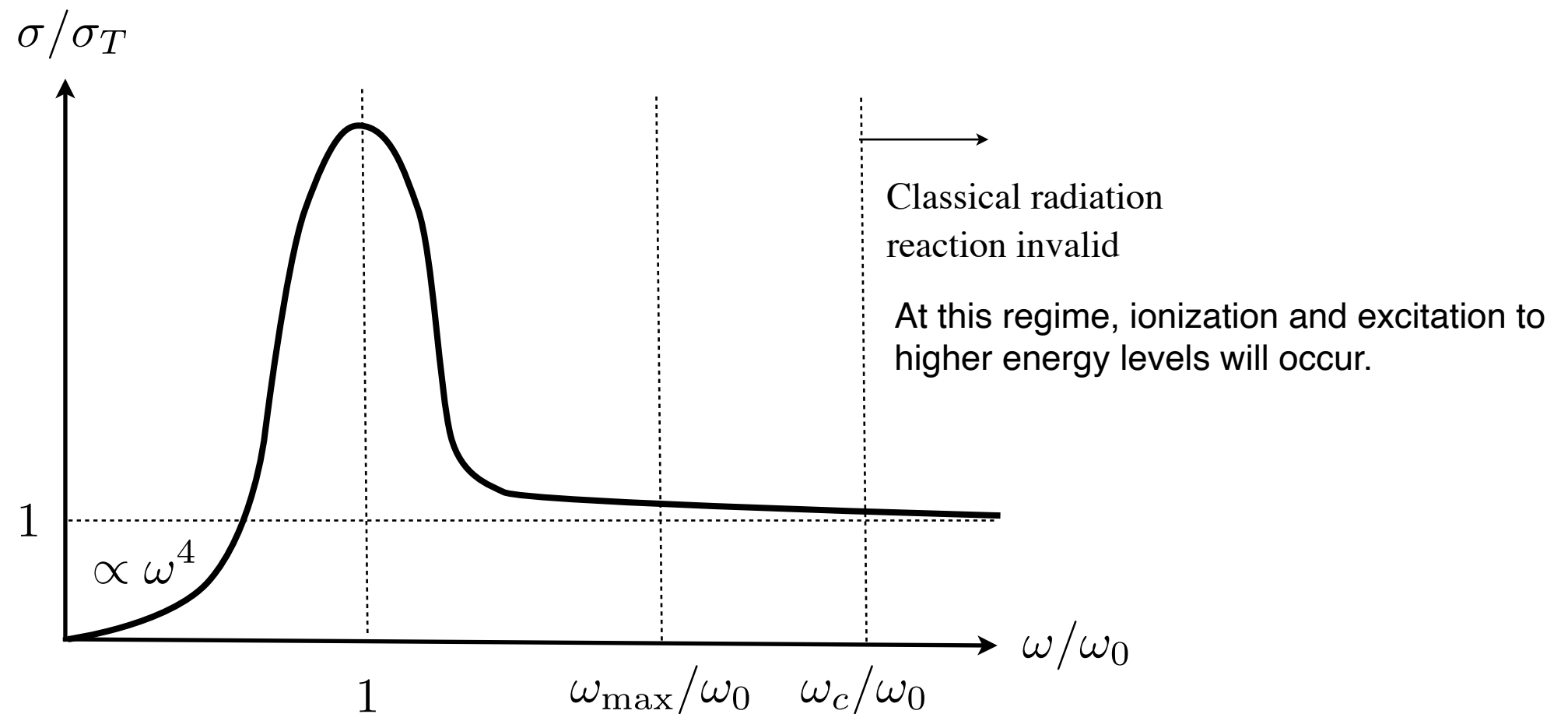
- Time-averaged total power radiated is given by

$$\begin{aligned} P &= \left\langle \frac{dW}{dt} \right\rangle = \frac{2e^2 \langle |\ddot{\mathbf{x}}|^2 \rangle}{3c^3} = \frac{e^2 \omega^4 |\mathbf{x}_0|^2}{3c^3} \\ &= \frac{e^4 E_0^2}{3m^2 c^3} \frac{\omega^4}{(\omega^2 - \omega_0^2)^2 + (\omega\gamma)^2} \end{aligned}$$

- Scattering cross section:

$$\sigma_{\text{sca}} \equiv \frac{\langle P \rangle}{\langle S \rangle}, \quad \langle S \rangle = \frac{c}{8\pi} E_0^2 \quad \longrightarrow \quad \sigma_{\text{sca}}(\omega) = \frac{8\pi e^4}{3m^2 c^4} \frac{\omega^4}{(\omega^2 - \omega_0^2)^2 + (\omega\gamma)^2}$$

$$= \sigma_T \frac{\omega^4}{(\omega^2 - \omega_0^2)^2 + (\omega\gamma)^2}$$



- Limiting Cases of Interest

(a) $\omega \gg \omega_0$ (Thomson scattering by free electron)

$$\sigma_{\text{sca}} = \sigma_T = \frac{8\pi}{3} r_e^2$$

- ▶ At high incident energies, the binding becomes negligible. Therefore, this corresponds to the case of a free electron.

(b) $\omega \ll \omega_0$ (Rayleigh scattering by bound electron)

$$\sigma_{\text{sca}} = \sigma_T \left(\frac{\omega}{\omega_0} \right)^4 = \sigma_T \left(\frac{\lambda_0}{\lambda} \right)^4$$

- ▶ Rayleigh scattering refers to the ***scattering of light by particles smaller than the wavelength of the light.***
- ▶ The strong wavelength dependence of the scattering means that shorter (blue) wavelengths are scattered more strongly than longer wavelengths.
- ▶ (blue color of the sky) The dependence results in the indirect blue light coming from all regions of the sky.
- ▶ (red color of the sun at sunset) Conversely, glancing toward the Sun, the colors that were not scattered away - the longer wavelengths such as red and yellow light - are directly visible, giving the Sun itself a slightly yellowish color.
- ▶ However, viewed from space, the sky is black and the Sun is white.

[2] Absorption/Scattering : Line Profile

(c) $\omega \approx \omega_0$ (resonance scattering of line radiation)

$$\begin{aligned}\sigma_{\text{sca}}(\omega) &\approx \sigma_T \frac{\omega_0^4}{(\omega - \omega_0)^2(2\omega_0)^2 + (\omega_0\gamma)^2} \\ &= \sigma_T \frac{\omega_0^2/4}{(\omega - \omega_0)^2 + (\gamma/2)^2} \\ \sigma_T \frac{\omega_0^2}{4} &= \frac{8\pi}{3} \left(\frac{e^2}{mc^2} \right)^2 \times \frac{1}{4} \times \left(\gamma \frac{3}{2} \frac{mc^3}{e^2 \omega_0^2} \right) = 2\pi^2 \frac{e^2}{mc} (\gamma/2\pi)\end{aligned}$$

Note that $\nu = 2\pi\omega$ and $\sigma_\nu = \sigma_\omega/2\pi$.

$$\begin{aligned}\sigma_\omega &= \frac{2\pi^2 e^2}{mc} \frac{\gamma/2\pi}{(\omega - \omega_0)^2 + (\gamma/2\pi)^2} \\ \sigma_\nu &= \frac{\pi e^2}{mc} \frac{\gamma/4\pi^2}{(\nu - \nu_0)^2 + (\gamma/4\pi)^2}\end{aligned}$$

- ▶ In the neighborhood of the resonance, ***the shape of the absorption/scattering cross-section is the same as the (spontaneous) emission line profile from the free oscillator. We already obtained the same conclusion, in the previous lecture.***
- ▶ Total scattering cross section is
- **Resonance line**
 - A spectral line caused by an electron jumping between the ground state and the first energy level in an atom or ion. It is the longest wavelength line produced by a jump to or from the ground state.
 - Because the majority of electrons are in the ground state in many astrophysical environments, and because the energy required to reach the first level is the least needed for any transition, resonance lines are the strongest lines in the spectrum for any given atom or ion.

$$\int_0^\infty \sigma_\nu d\nu = \frac{\pi e^2}{mc}$$

- ***In the quantum theory of spectral lines,***

we obtain similar formulas, which are conveniently stated in terms of the classical results as

$$\sigma_\nu = f_{nn'} \frac{\pi e^2}{mc} \frac{\gamma/4\pi^2}{(\nu - \nu_0)^2 + (\gamma/4\pi)^2}$$

$$\int_0^\infty \sigma_\nu d\nu = f_{nn'} \frac{\pi e^2}{mc}$$

where $f_{nn'}$ is called the **oscillator strength** or **f-value** for the transition between states n and n' .

Selected Resonance Lines^a with $\lambda < 3000 \text{ \AA}$

| | Configurations | ℓ | u | $E_\ell/hc(\text{ cm}^{-1})$ | $\lambda_{\text{vac}}(\text{ \AA})$ | $f_{\ell u}$ |
|--------|----------------------------|---------------|---------------|------------------------------|-------------------------------------|--------------|
| C IV | $1s^2 2s - 1s^2 2p$ | $^2S_{1/2}$ | $^2P_{1/2}^o$ | 0 | 1550.772 | 0.0962 |
| | | $^2S_{1/2}$ | $^2P_{3/2}^o$ | 0 | 1548.202 | 0.190 |
| N V | $1s^2 2s - 1s^2 2p$ | $^2S_{1/2}$ | $^2P_{1/2}^o$ | 0 | 1242.804 | 0.0780 |
| | | $^2S_{1/2}$ | $^2P_{3/2}^o$ | 0 | 1242.821 | 0.156 |
| O VI | $1s^2 2s - 1s^2 2p$ | $^2S_{1/2}$ | $^2P_{1/2}^o$ | 0 | 1037.613 | 0.066 |
| | | $^2S_{1/2}$ | $^2P_{3/2}^o$ | 0 | 1037.921 | 0.133 |
| C III | $2s^2 - 2s 2p$ | 1S_0 | $^1P_1^o$ | 0 | 977.02 | 0.7586 |
| C II | $2s^2 2p - 2s 2p^2$ | $^2P_{1/2}^o$ | $^2D_{3/2}^o$ | 0 | 1334.532 | 0.127 |
| | | $^2P_{3/2}^o$ | $^2D_{5/2}^o$ | 63.42 | 1335.708 | 0.114 |
| N III | $2s^2 2p - 2s 2p^2$ | $^2P_{1/2}^o$ | $^2D_{3/2}^o$ | 0 | 989.790 | 0.123 |
| | | $^2P_{3/2}^o$ | $^2D_{5/2}^o$ | 174.4 | 991.577 | 0.110 |
| CI | $2s^2 2p^2 - 2s^2 2p 3s$ | 3P_0 | $^3P_1^o$ | 0 | 1656.928 | 0.140 |
| | | 3P_1 | $^3P_2^o$ | 16.40 | 1656.267 | 0.0588 |
| | | 3P_2 | $^3P_2^o$ | 43.40 | 1657.008 | 0.104 |
| N II | $2s^2 2p^2 - 2s 2p^3$ | 3P_0 | $^3D_1^o$ | 0 | 1083.990 | 0.115 |
| | | 3P_1 | $^3D_2^o$ | 48.7 | 1084.580 | 0.0861 |
| | | 3P_2 | $^3D_3^o$ | 130.8 | 1085.701 | 0.0957 |
| NI | $2s^2 2p^3 - 2s^2 2p^2 3s$ | $^4S_{3/2}^o$ | $^4P_{5/2}$ | 0 | 1199.550 | 0.130 |
| | | $^4S_{3/2}^o$ | $^4P_{3/2}$ | 0 | 1200.223 | 0.0862 |
| OI | $2s^2 2p^4 - 2s^2 2p^3 3s$ | 3P_2 | $^3S_1^o$ | 0 | 1302.168 | 0.0520 |
| | | 3P_1 | $^3S_1^o$ | 158.265 | 1304.858 | 0.0518 |
| | | 3P_0 | $^3S_1^o$ | 226.977 | 1306.029 | 0.0519 |
| Mg II | $2p^6 3s - 2p^6 3p$ | $^2S_{1/2}$ | $^2P_{1/2}^o$ | 0 | 2803.531 | 0.303 |
| | | $^2S_{1/2}$ | $^2P_{3/2}^o$ | 0 | 2796.352 | 0.608 |
| Al III | $2p^6 3s - 2p^6 3p$ | $^2S_{1/2}$ | $^2P_{1/2}^o$ | 0 | 1862.790 | 0.277 |
| | | $^2S_{1/2}$ | $^2P_{3/2}^o$ | 0 | 1854.716 | 0.557 |

Table 9.4 in [Draine]

See also Table 9.3

[3] Line Broadening Mechanisms

- **Atomic levels are not infinitely sharp**, nor are the lines connecting them.
 - (1) Doppler (Thermal) Broadening
 - (2) Natural Broadening
 - (3) Collisional Broadening
 - (4) Thermal Doppler + Natural Broadening
- **[1] Doppler (Thermal) Broadening**
 - The simplest mechanism for line broadening in the Doppler effect. An atom is in thermal motion, so that the frequency of emission or absorption in its own frame corresponds to a different frequency for an observer.
 - Each atom has its own Doppler shift, so that the net effect is to spread the line out, but not to change its total strength.
 - The change in frequency associated with an atom with velocity component v_z along the line of sight (say, z axis) is, to lowest order in v_z/c , given by

$$\nu - \nu_0 = \nu_0 \frac{v_z}{c}$$

Recall Doppler shift: $\left[\frac{\nu}{\nu_0} = \frac{1}{\gamma(1 - \beta \cos \theta)} \rightarrow \nu \approx \nu_0 (1 + \beta \cos \theta) \rightarrow \nu - \nu_0 = \frac{\nu_0 v_z}{c} \right]$

- Here, ν_0 is the rest-frame frequency.

-
- We need to consider the velocity distribution of atoms. The number of atoms having velocities in the range $(v_z, v_z + dv_z)$ is proportional to

$$f(v_z)dv_z = \exp\left(-\frac{mv_z^2}{2kT}\right)dv_z$$

- From the Doppler shift formula, we have

$$v_z = \frac{c(\nu - \nu_0)}{\nu_0} \rightarrow dv_z = \frac{cd\nu}{\nu_0}$$

- Therefore, the strength of the emission is proportional to

$$\exp\left(-\frac{mv_z^2}{2kT}\right)dv_z \propto \exp\left[-\frac{mc^2(\nu - \nu_0)^2}{2\nu_0^2 kT}\right]d\nu$$

- Then, the normalized profile function is

$$\left(v_{\text{rms}} = \sqrt{\frac{kT}{m}} \right)$$

$$\phi(\nu) = \frac{1}{\Delta\nu_D \sqrt{\pi}} e^{-(\nu - \nu_0)^2 / (\Delta\nu_D)^2} \quad \text{where} \quad \Delta\nu_D = \nu_0 \frac{v_{\text{th}}}{c} \quad \text{is the Doppler width.}$$

$$= \frac{\nu_0}{c} \sqrt{\frac{2kT}{m}} = \nu_0 \frac{\sqrt{2}v_{\text{rms}}}{c}$$

-
- Numerical value of the velocity broadening is

$$v_{\text{th}} = \left(\frac{2k_{\text{B}}T}{m} \right)^{1/2} = 1.3 \text{ km s}^{-1} \left(\frac{T}{100 \text{ K}} \right)^{1/2} \left(\frac{m}{m_{\text{H}}} \right)^{-1/2}$$

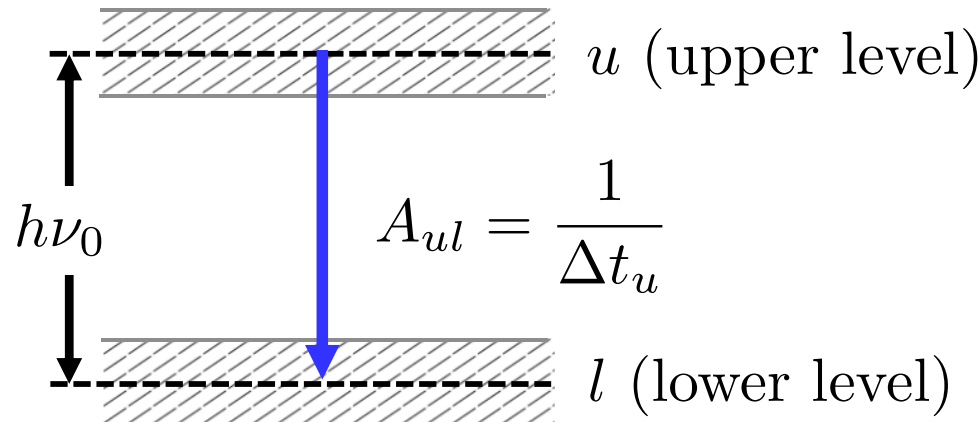
- In addition to thermal motions, there can be turbulent velocities associated with macroscopic velocity fields. The turbulent motions are accounted for by an effective Doppler width.

$$\Delta\nu_{\text{D}} = \nu_0 \frac{b}{c}$$
$$b \equiv (v_{\text{th}}^2 + v_{\text{turb}}^2)^{1/2}$$

where v_{turb} is $\sqrt{2}$ times a root-mean-square measure of the turbulent velocities. This assumes that the turbulent velocities also have a Gaussian distribution.

• [2] Natural Broadening

- The intrinsic line width of a line is due to ***the Heisenberg uncertainty principle***. If an energy level u has a lifetime Δt , then uncertainty (spread) in energy ΔE must be $\Delta E \sim \hbar/\Delta t$ ($\hbar = h/2\pi$), and the resulting spread in the frequency of emitted photons is $\Delta\nu = \Delta E/h$.



A_{ul} = decay rate
= decay probability per unit time, Einstein A coefficient.

ΔE_u = uncertainty in energy of u

Δt_u = the uncertainty in time of occupation of u

$\Delta\nu_u$ = uncertainty in frequency

$$= \Delta E_u/h = 1/(2\pi\Delta t_u) = A_{ul}/(2\pi) \longrightarrow$$

$$\phi_\nu = \frac{\gamma/4\pi^2}{(\nu - \nu_0)^2 + (\gamma/4\pi)^2}$$

In terms of the line width $\Delta\nu_u$, the line profile can be rewritten as

$$\phi_\nu = \frac{1}{2\pi} \frac{\Delta\nu_u/2}{(\nu - \nu_0)^2 + (\Delta\nu_u/2)^2}$$

FWHM of the Lorentz function:
 $\Delta\nu_u = \gamma/2\pi$

Therefore, γ is equivalent to the Einstein A-coefficient., i.e., $\gamma = A_{ul}$.

-
- The intrinsic line width is $\gamma = A_{ul}$.
 - This means forbidden lines are intrinsically narrower than permitted lines.
 - For instance, the permitted Ly α line has $A_{ul}/\nu_{ul} \sim 3 \times 10^{-7}$, while the forbidden [OIII] 5007Å has a tiny width $A_{ul}/\nu_{ul} \sim 3 \times 10^{-17}$.
 - The intrinsic line width of [O III] 5007Å is equivalent to the Doppler broadening of $\Delta v \sim 3 \times 10^{-17} c \sim 10 \text{ nm s}^{-1} \sim 30 \text{ cm yr}^{-1}$
 - For a multiple-level absorber, the upper and lower can both be broadened by transitions to other levels.

$$\gamma_{ul} = \sum_{E_j < E_u} A_{uj} + \sum_{E_j < E_\ell} A_{\ell j}$$

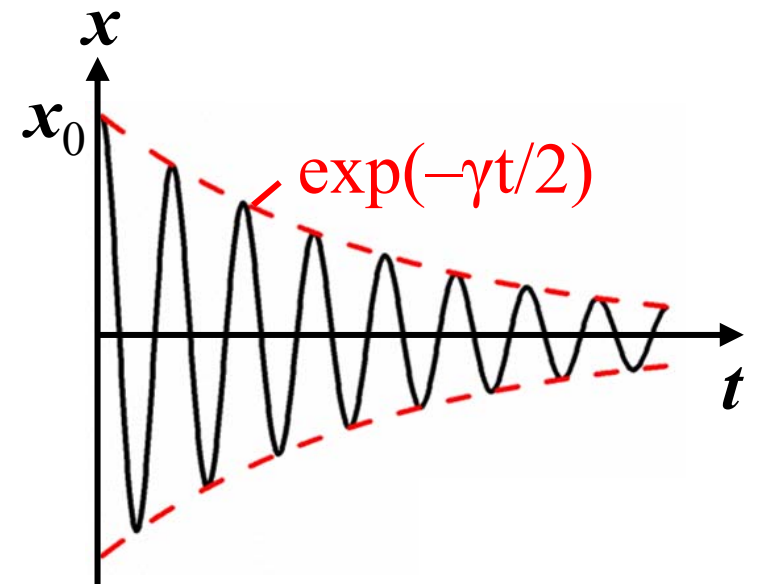
- For Ly α ($n = 1-2$), $\gamma_{ul} = A_{21} = 6.3 \times 10^8 \text{ s}^{-1}$
 $\Delta\nu/\nu \sim 4 \times 10^{-8}$
- For H α ($n = 2-3$), $\gamma_{ul} = A_{32} + A_{31} + A_{21} = 8.9 \times 10^8 \text{ s}^{-1}$
 $\Delta\nu/\nu \sim 3 \times 10^{-7}$

Suppose that the electric field is of the form $e^{-\gamma t/2}$ and then the energy decays proportional to $e^{-\gamma t}$.

We then have an emitted spectrum determined by the decaying sinusoid type of electric field.

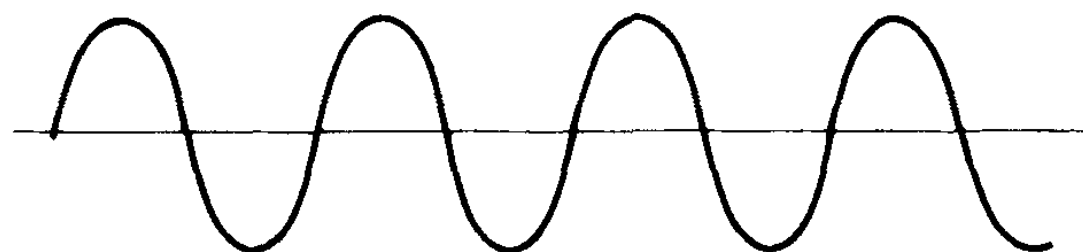
Its Fourier transform (spectral profile) is a Lorentz (or natural, or Cauchy) profile:

$$\phi_\nu = \frac{\gamma/4\pi^2}{(\nu - \nu_0)^2 + (\gamma/4\pi)^2}$$

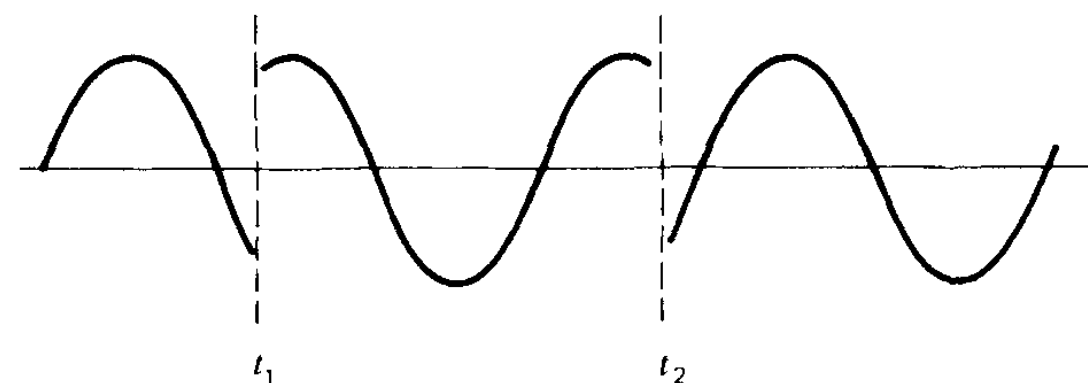


- [3] Collisional Broadening (or Pressure Broadening)
 - The Lorentz profile applies even to certain types of collisional broadening mechanisms.
 - If the atom suffers collisions with other particles while it is emitting, the phase of the emitted radiation can be altered suddenly. If the phase changes completely randomly at the collision times, then information about the emitting frequencies is lost.
 - If the collisions occur with frequency ν_{col} , that is, each atom experiences ν_{col} collisions per unit time on the average, then the profile is

$$\phi_\nu = \frac{\Gamma/4\pi^2}{(\nu - \nu_0)^2 + (\Gamma/4\pi)^2} \quad \text{where} \quad \Gamma = \gamma + 2\nu_{\text{col}}$$



purely sinusoidal



random phase interruptions
by atomic collisions

• [4] Voigt profile : Thermal + Natural broadening

- Atoms shows both a Lorentz profile plus the Doppler effect. In this case, we can write the profile as an average of the Lorentz profile over the various velocity states of the atom:

Maxwell distribution: $f_{v_z} = \frac{1}{\pi^{1/2} (2kT/m)^{1/2}} \exp(-mv_z^2/2kT) \longrightarrow f_y = \frac{1}{\pi^{1/2}} \exp(-y^2)$

$$v_{\text{th}} \equiv \sqrt{\frac{2kT}{m}}, \quad y \equiv \frac{v_z}{v_{\text{th}}}$$

To interact with an atom with velocity v_z , the photon central frequency should be $\nu_0 + \nu_0(v_z/c)$. Then, the Lorentz profile at the frequency $\nu' = \nu - [\nu_0 + \nu_0(v_z/c)] = (\nu - \nu_0) - \nu_0(v_{\text{th}}/c)y$ is supposed to be multiplied with the Maxwell distribution.

Change of variables for the Lorentz function: $\phi_y^L = \phi_\nu^L \left| \frac{d\nu}{dy} \right| = \phi_\nu^L \times \left(\nu_0 \frac{v_{\text{th}}}{c} \right)$

Let $\Delta\nu_D \equiv \nu_0 \frac{v_{\text{th}}}{c}$, $u \equiv \frac{\nu - \nu_0}{\Delta\nu_D} = \frac{\nu - \nu_0}{\nu_0} \frac{c}{v_{\text{th}}}$, $a = \frac{\Gamma/4\pi}{\Delta\nu_D}$

$$\begin{aligned} \phi(\nu) &= \int_{-\infty}^{\infty} \phi_y^L f_y dy \\ &= \int_{-\infty}^{\infty} \left(\nu_0 \frac{v_{\text{th}}}{c} \right) \frac{\Gamma/4\pi^2}{[(\nu - \nu_0) - \nu_0(v_{\text{th}}/c)y]^2 + (\Gamma/4\pi)^2} \left(\frac{1}{\pi^{1/2}} \right) \exp(-y^2) dy \\ &= \frac{a}{\pi^{3/2} \Delta\nu_D} \int_{-\infty}^{\infty} \frac{e^{-y^2}}{(u - y)^2 + a^2} dy \end{aligned}$$

- The profile can be written using the Voigt function.

$$\phi(\nu) = \frac{1}{\Delta\nu_D \sqrt{\pi}} H(u, a)$$

Here, a is a ratio of the intrinsic broadening to the thermal broadening.

u is a measure of how far you are from the line center, in units of thermal broadening parameter.

In terms of Doppler velocity, u can be expressed as

$$u = \frac{\nu - \nu_0}{\Delta\nu_D} = \frac{\nu - \nu_0}{\nu_0} \frac{c}{v_{\text{th}}}$$

In the velocity term,

$$u = \frac{v}{v_{\text{th}}}, \text{ where } v = \frac{\nu - \nu_0}{\nu_0} c$$

Voigt-Hjerting function:

$$H(u, a) \equiv \frac{a}{\pi} \int_{-\infty}^{\infty} \frac{e^{-y^2} dy}{(u - y)^2 + a^2}$$

$$a \equiv \frac{\Gamma}{4\pi\Delta\nu_D}$$

$$u \equiv \frac{\nu - \nu_0}{\Delta\nu_D}$$

$$\Delta\nu_D = \frac{\nu_0}{c} \sqrt{\frac{2kT}{m}}$$

Including the turbulent motion

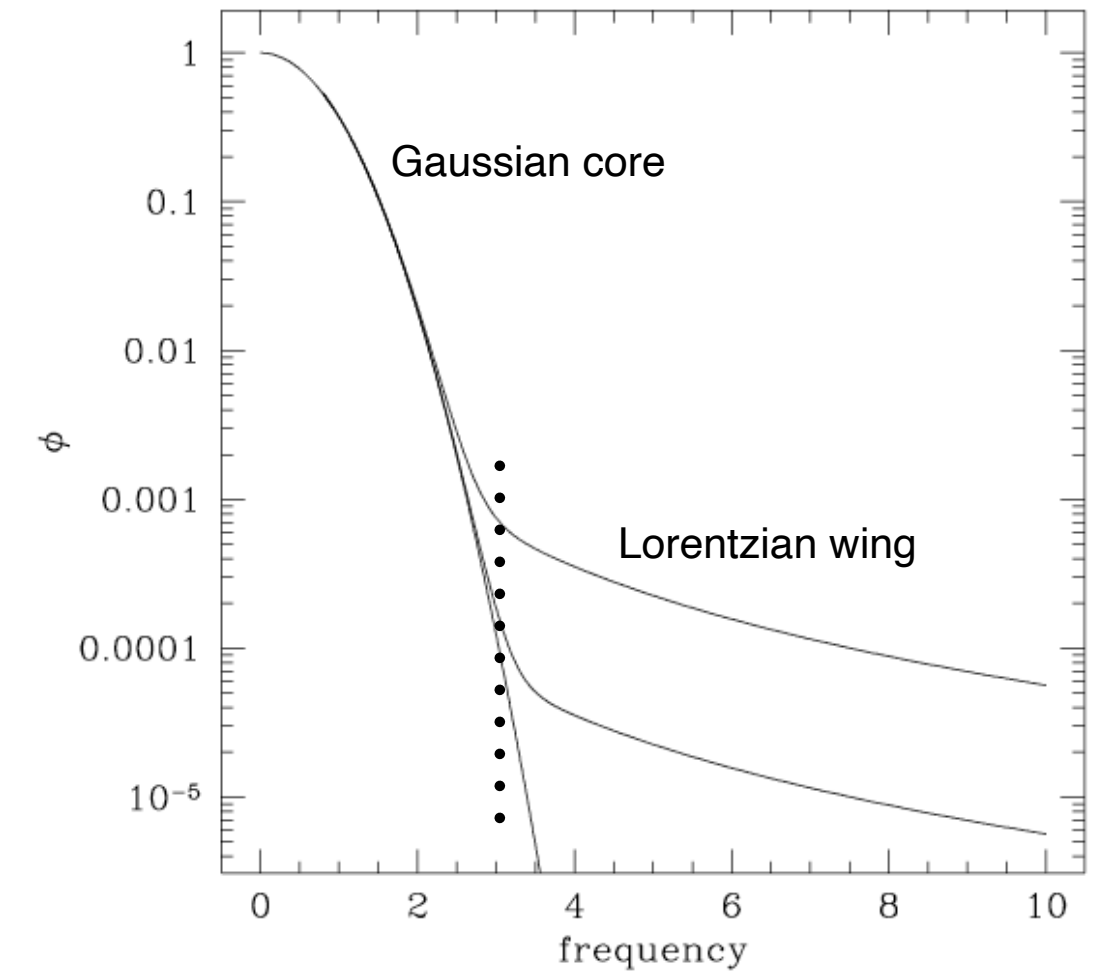
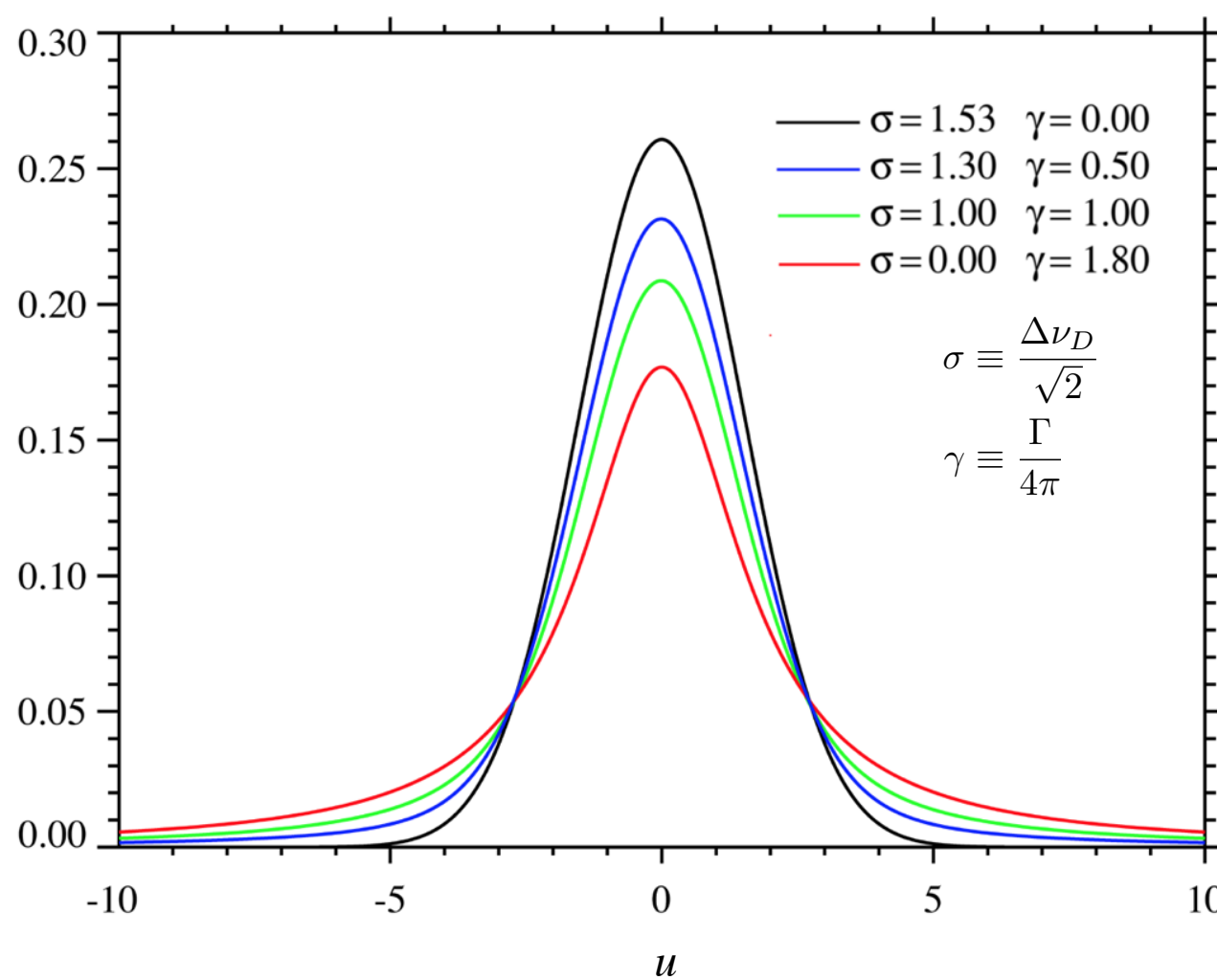
$$\Delta\nu_D = \nu_0 \frac{v_{\text{th}}}{c} \rightarrow \Delta\nu_D = \nu_0 \frac{b}{c}$$

$$\text{where } b = \sqrt{v_{\text{th}}^2 + v_{\text{turb}}^2}, \quad v_{\text{th}} = \sqrt{\frac{2kT}{m}}$$

Properties of Voigt Function

- For small a , the “core” of the line is dominated by the Gaussian (Doppler) profile, whereas the “wings” are dominated by the Lorentz profile.

$$H(a, u) \equiv \frac{a}{\pi} \int_{-\infty}^{\infty} \frac{e^{-y^2} dy}{(u - y)^2 + a^2}$$



- In most case, $a \ll 1$. For Ly α at $T = 100$ K, $a \sim 0.05$.

- Line center:

$$H(0, a) = \exp(a^2) \operatorname{Erfc}(a) \approx 1 - \frac{2}{\sqrt{\pi}}a + a^2 - \mathcal{O}(a^3)$$

- Taylor series Expansion of the Voigt function :

$$H(a, u) \equiv \frac{a}{\pi} \int_{-\infty}^{\infty} \frac{e^{-y^2} dy}{(u - y)^2 + a^2}$$

- Near the line center ($u \rightarrow 0$), the contribution to the integral is dominated by $y = u$. Therefore,

$$H(a, u) \simeq \frac{a}{\pi} e^{-u^2} \int_{-\infty}^{\infty} \frac{dy}{y^2 + a^2} = e^{-u^2}$$

which is known as the Doppler core.

- In the line wings away from the core ($u \gg 1$), the integral is dominated by $y \sim 0$ because of the rapidly decreasing function in the numerator.

$$H(a, u) \simeq \frac{a}{\pi} \int_{-\infty}^{\infty} \frac{e^{-y^2} dy}{u^2} = \frac{a}{\pi} \frac{\sqrt{\pi}}{u^2} = \frac{a}{\sqrt{\pi} u^2}$$

- In summary, we obtain the Voigt function in a Taylor series expansion around $a = 0$.

$$H(u, a) \approx H(u, 0) + a \left. \frac{dH}{da} \right|_{a=0} \approx e^{-u^2} + a \frac{1}{\sqrt{\pi} u^2}$$

- The first term represents the Gaussian core, provided by the thermal broadening, and the second term represents the Lorentizan damping wing.
- Transition from Doppler core to damping wing can be found by solving:

$$e^{u^2} = \frac{\sqrt{\pi}}{a} u^2 \quad \rightarrow \quad u^2 = \ln \left(\frac{\sqrt{\pi}}{a} \right) + \ln u^2 \quad \text{for hydrogen}$$

$$b = 13 \text{ km s}^{-1} (T/10^4 \text{ K})^{1/2}$$

- The solution for this transcendental equation for Ly α is

$$u^2 \approx 10.31 + \ln \left[\left(\frac{6.265 \times 10^8 \text{ s}^{-1}}{\gamma_{ul}} \right) \left(\frac{1215.67 \text{ \AA}}{\lambda_{ul}} \right) \left(\frac{b}{10 \text{ km s}^{-1}} \right) \right]$$

provided that the quantity in square brackets is not very large or very small. The damping wing for $|u| \gtrsim 3.2$ or velocity shifts $|v| \gtrsim 3.2 (b/10 \text{ km s}^{-1})$.

Optical Depth

- The optical depth in an absorption line can be written

$$\tau_\nu = \frac{\pi e^2}{m_e c} f_{\ell u} \left(1 - \frac{n_u/g_u}{n_\ell/g_\ell} \right) N_\ell \phi_\nu$$

Here, $N_\ell \equiv \int n_\ell ds$ is the column density of the absorbers.

The line profile is given by $\phi_\nu = \frac{1}{\Delta\nu_D \sqrt{\pi}} H(u, a)$, and its value at the line center is

$$\begin{aligned} \phi_\nu(\nu = \nu_{\ell u}) &= \frac{1}{\nu_{\ell u}(b/c)\sqrt{\pi}} H(0, a) \\ &\approx \frac{1}{\nu_{\ell u}(b/c)\sqrt{\pi}} \end{aligned}$$

$$\begin{aligned} u &= \frac{\nu - \nu_{\ell u}}{\Delta\nu_D} = \frac{\nu - \nu_{u\ell}}{\nu_{\ell u}(b/c)} \\ &= \frac{v}{b} \quad \left(v = \frac{\nu - \nu_{\ell u}}{\nu_{\ell u}} c, b = \sqrt{2}\sigma_v = \sqrt{\frac{2k_B T}{m}} \right) \end{aligned}$$

The correction factor for stimulated emission is negligible for the optical lines. Then, dropping the correction factor, the optical depth can be written

$$\tau_\nu = \tau_0 H(u, a)$$

Here, τ_0 is the optical depth at the line center.

$$\tau_0 = \frac{\sqrt{\pi}e^2}{m_e c} f_{\ell u} \frac{\lambda_{\ell u}}{b} N_\ell$$

-
- The central optical depth for Ly α is

$$\tau_0 = 0.7580 \left(\frac{N_\ell}{10^{13} \text{ cm}^{-2}} \right) \left(\frac{f_{\ell u}}{0.4164} \right) \left(\frac{\lambda_{\ell u}}{1215.67 \text{ \AA}} \right) \left(\frac{10 \text{ km s}^{-1}}{b} \right)$$

- In the WNM, Ly α will be optically thin ($\tau_0 < 1$) when $N_\ell < 10^{13} \text{ cm}^{-2}$ and optically thick ($\tau_0 > 1$) when $N_\ell > 10^{13} \text{ cm}^{-2}$.
- In the CNM, Ly α will be optically thin when $N_\ell < 10^{12} \text{ cm}^{-2}$ and optically thick when $N_\ell > 10^{12} \text{ cm}^{-2}$.
- In Milky Way, the total column density of hydrogen atom is $N_\ell \sim 10^{20} \text{ cm}^{-2}$.
- The column density of the Earth's atmosphere, looking upward from sea level, is $N \sim 2 \times 10^{25} \text{ cm}^{-2}$

Absorption Line Shapes

- Lyman α absorption line profiles for $b = 10 \text{ km s}^{-1}$

$$F_\nu/F_\nu(0) = e^{-\tau_0 H(u,a)}$$

- When $\tau_0 < 1$, $F_\nu/F_\nu(0) \approx 1 - \tau_\nu$ and thus the shape of an absorption line resembles an upside-down Voight function.
- When $\tau_0 \gg 1$, the absorption line saturates at its center and becomes increasingly “box-shaped.”

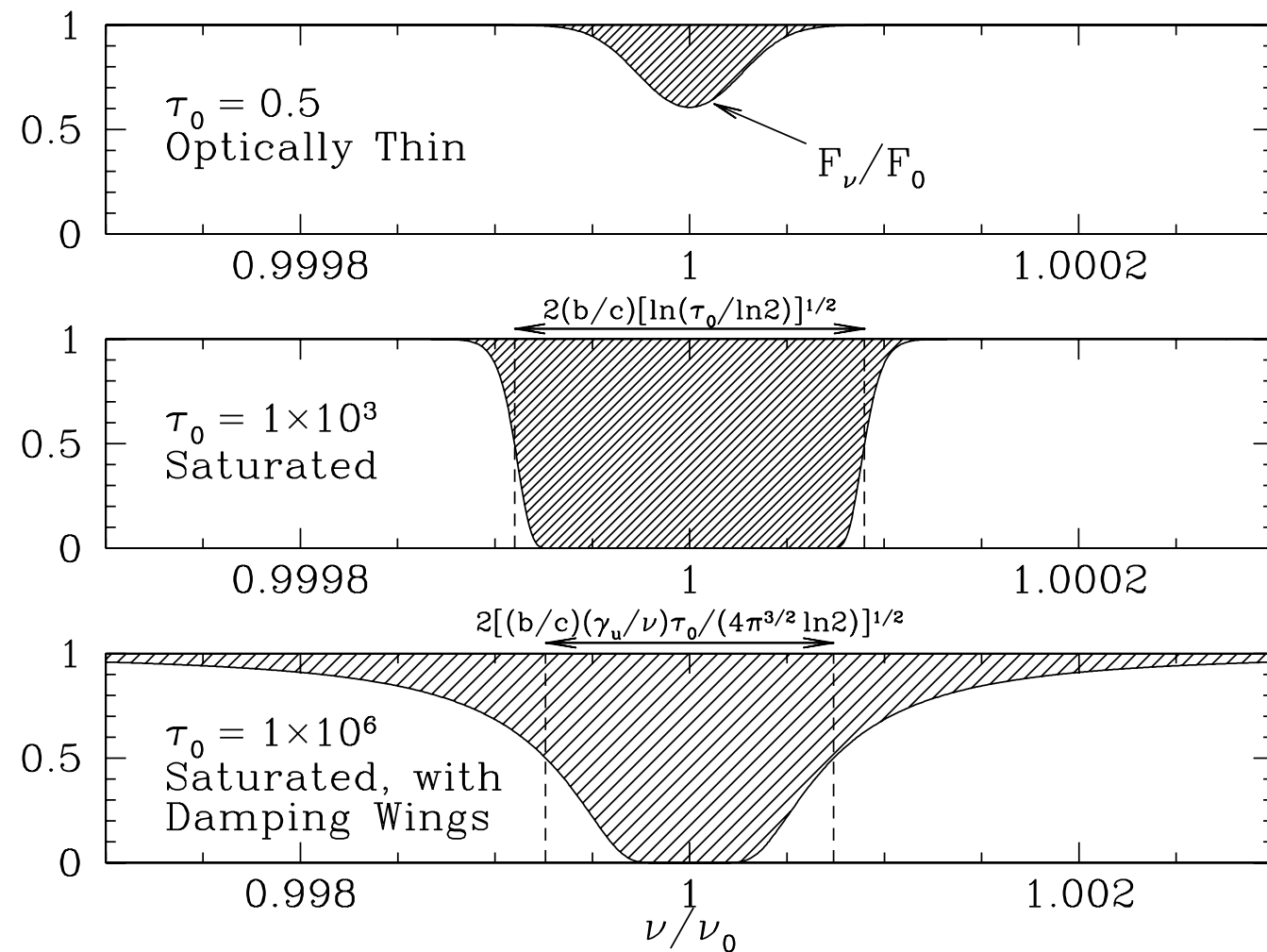


Figure 9.1 in [Draine]

Note the different abscissa in the lowest panel.

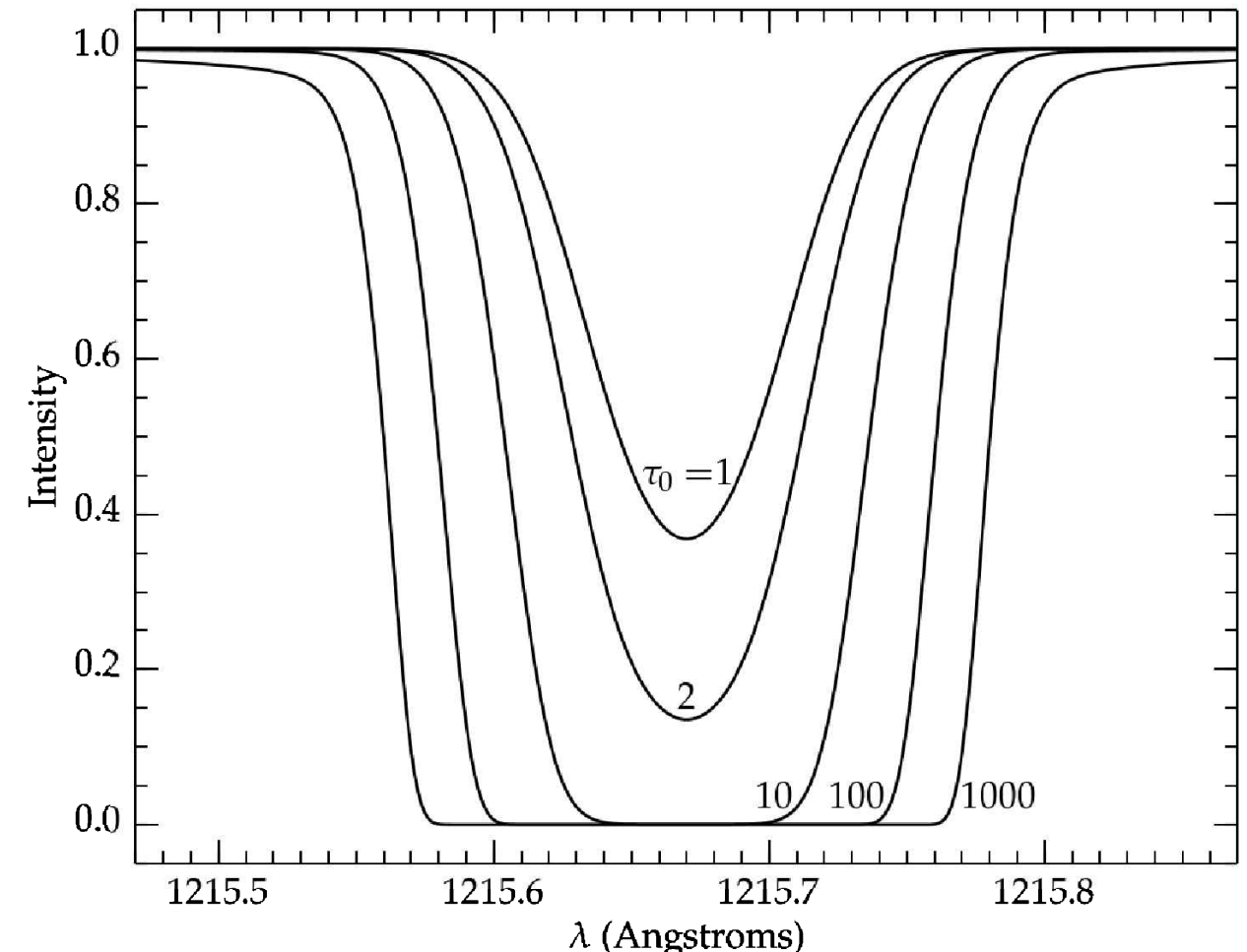


Figure 9.1 in [Ryden]

Equivalent Width & Curve of growth

- ***Equivalent width***
 - The spectrograph often lack the spectral resolution to resolve the profiles of narrow lines, but can measure the total amount of “missing power” resulting from a narrow absorption line.
 - The equivalent width is a measure of the strength of an absorption line, in terms of “missing power” in the unresolved absorption line.
- ***Curve of growth***
 - The curve of growth refers to the numerical relation between the observed equivalent width and the underlying optical depth (or the column density) of the absorber.

Equivalent Width

- Suppose that we measure the energy flux density F_ν using an aperture of solid angle $\Delta\Omega$. Then, we obtain the flux density at the observer:

$$F_\nu = F_\nu(0)e^{-\tau_\nu} + B_\nu(T_{\text{exc}})\Delta\Omega(1 - e^{-\tau_\nu})$$

Here, $F_\nu(0)$ is the flux density of the background light source.

- At optical frequencies and in the neutral medium, nearly all atoms are in their ground state. Thus, we normally have $n_u/n_\ell \ll 1$, $B_\nu(T_{\text{exc}})\Delta\Omega \ll F_\nu(0)$. Then, we can neglect the emission from the ISM.



$$\frac{h\nu}{k_B T_{\text{exc}}} = \frac{6000 \text{ \AA}}{\lambda} \frac{2.4 \times 10^4 \text{ K}}{T_{\text{exc}}}$$

$$F_\nu = F_\nu(0)e^{-\tau_\nu}$$

- If the background spectrum is smooth, we can define the **dimensionless equivalent width** and the **wavelength equivalent width** as follows:

$$W \equiv \int \frac{d\nu}{\nu_0} \left[1 - \frac{F_\nu}{F_\nu(0)} \right] = \int \frac{d\nu}{\nu_0} (1 - e^{-\tau_\nu})$$

$$W_\lambda \equiv \int d\lambda (1 - e^{-\tau_\lambda}) \approx \lambda_0 W$$

- The equivalent width is the width of a straight-sided, perfectly black absorption line that has the same integrated flux deficit as the actual absorption line.

Overall Shape of the Curve of Growth

The Curve of Growth

= the relation between optical depth at line center and equivalent width

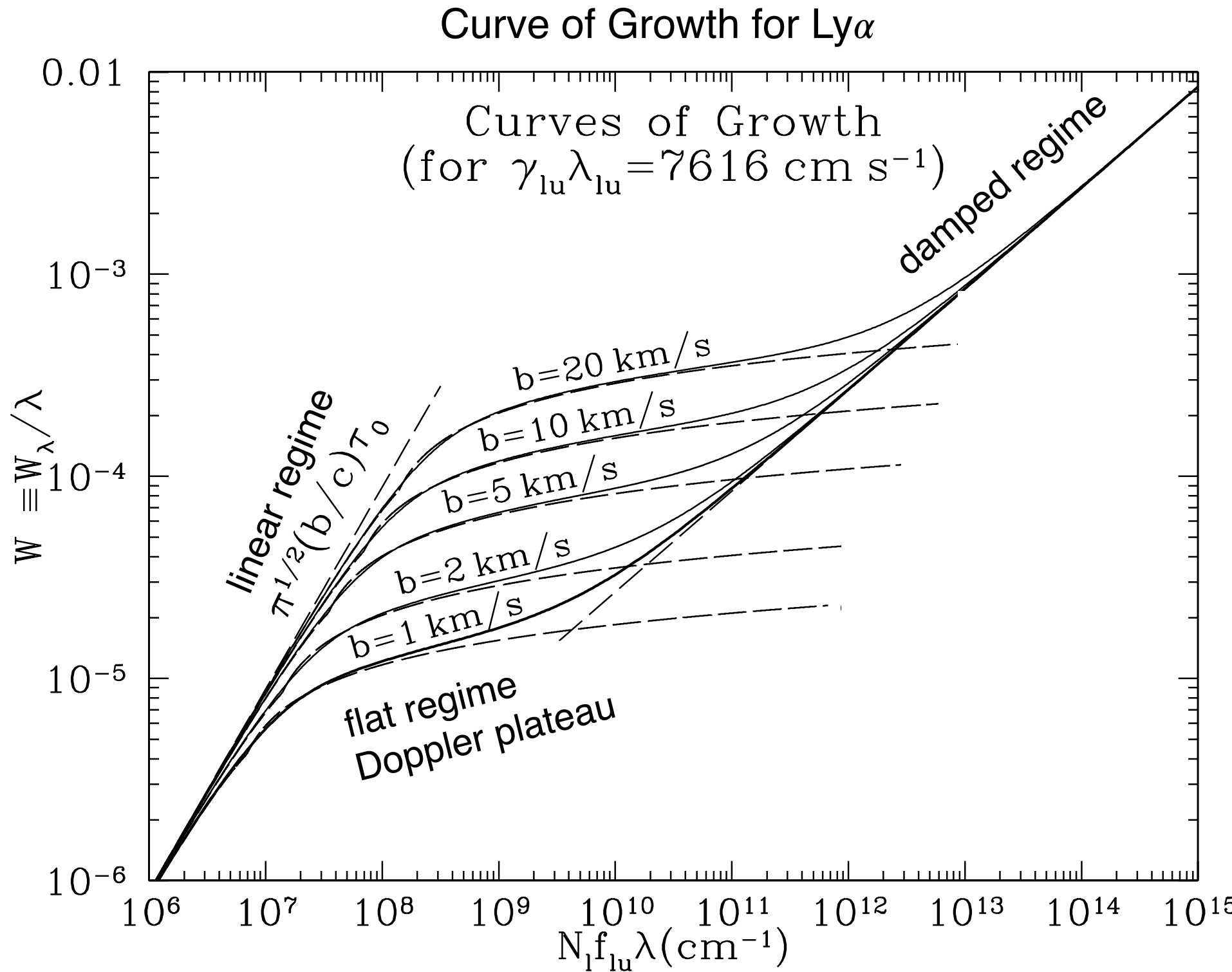


Figure 9.2 in [Draine]

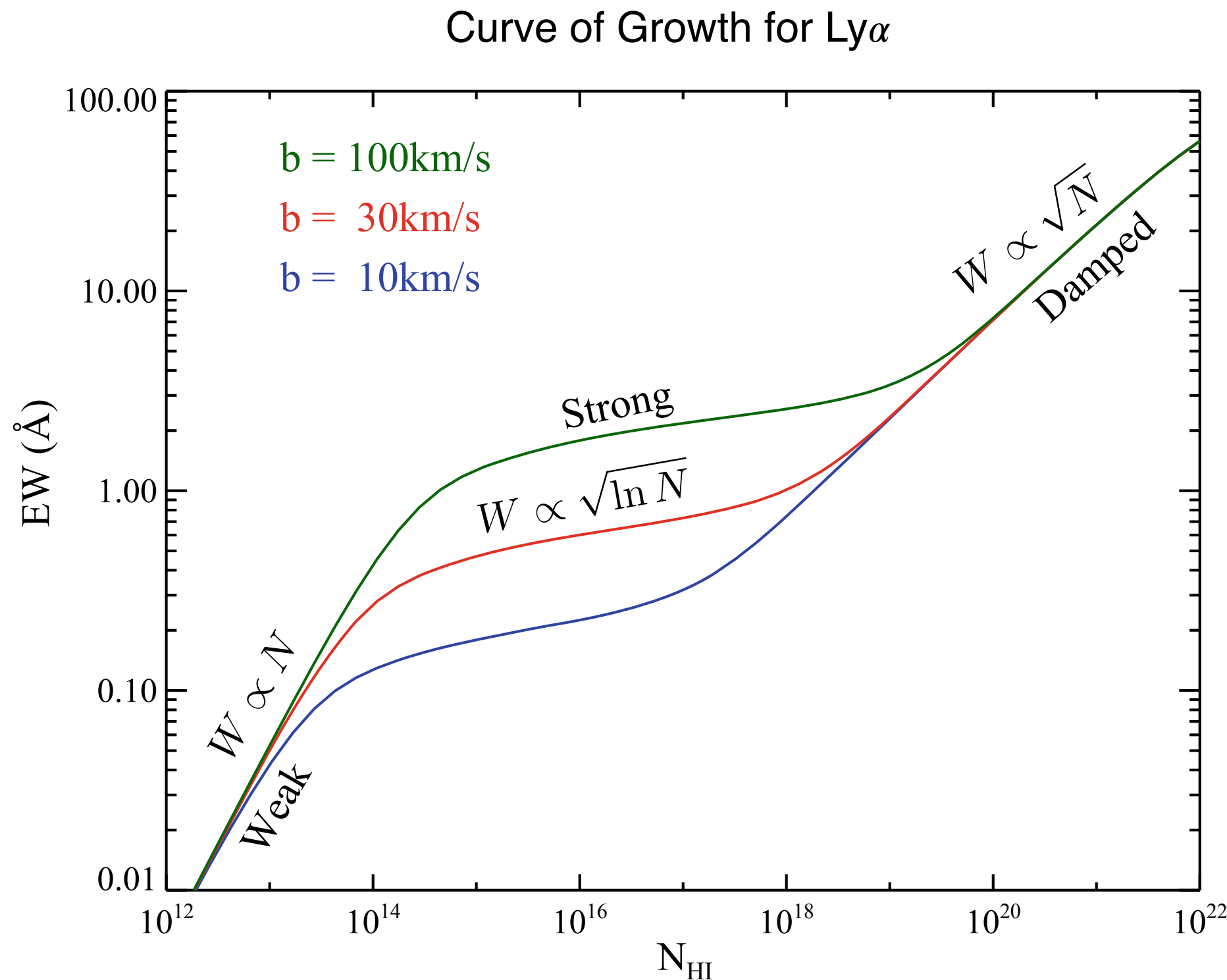


Figure 2.10 in Chap. 2 [Prochaska]
Lyman-alpha as An Astrophysical and Cosmological Tool

The Curve of Growth

- Equivalent width:

$$W = \int_{-\infty}^{\infty} \frac{d\nu}{\nu_0} (1 - e^{-\tau_\nu}) = \frac{b}{c} \int_{-\infty}^{\infty} du (1 - e^{-\tau_\nu})$$

- Optically Thin Absorption, $\tau_0 \lesssim 1$ (linear regime)**

$$\begin{aligned} W &= \frac{b}{c} \int_{-\infty}^{\infty} du \left(\tau_\nu - \frac{\tau_\nu^2}{2} + \dots \right) \approx \frac{b}{c} \int_{-\infty}^{\infty} du \left(\tau_0 e^{-u^2} - \tau_0^2 \frac{e^{-2u^2}}{2} + \dots \right) \\ &= \sqrt{\pi} \frac{b}{c} \tau_0 \left(1 - \frac{\tau_0}{2\sqrt{2}} + \dots \right) \end{aligned}$$

\uparrow $\tau_\nu = \tau_0 H(u, a) \approx \tau_0 e^{-u^2}$ if $a \ll 1$

$$\begin{aligned} W &\approx \sqrt{\pi} \frac{b}{c} \frac{\tau_0}{1 + \tau_0/(2\sqrt{2})} & \xleftarrow{\hspace{1cm}} & 1 - x \approx \frac{1}{1 + x} \\ &= \frac{\pi e^2}{m_e c^2} N_\ell f_{\ell u} \lambda_{\ell u} & \xleftarrow{\hspace{1cm}} & \tau_0 = \frac{\sqrt{\pi} e^2}{m_e c} f_{\ell u} \frac{\lambda_{\ell u}}{b} N_\ell \end{aligned}$$

$$W = 4.48 \times 10^{-6} \left(\frac{N_\ell}{10^{12} \text{ cm}^{-2}} \right) \left(\frac{f_{\ell u}}{0.4164} \right) \left(\frac{\lambda_{\ell u}}{1215.67 \text{ \AA}} \right)$$

$$N_\ell = 1.84 \times 10^{12} \text{ cm}^{-2} \left(\frac{0.4164}{f_{\ell u}} \right) \left(\frac{1215.67 \text{ \AA}}{\lambda_{\ell u}} \right)^2 \left(\frac{W_\lambda}{0.01 \text{ \AA}} \right) \text{ if } \tau_0 \lesssim 1$$

$$\leftarrow \quad W \approx \frac{W_\lambda}{\lambda_{\ell u}}$$

The measurement of W allows us to determine N , provided that the line is optical thin.

-
- **Flat Portion of the Curve of Growth,** $1 < \tau_0 \lesssim \tau_{\text{damp}}$
 - Now consider what happens when an absorption line is optically thick, but not so optically thick that the broad Lorentz wing ν^{-2} provide a significant contribution to the absorption.
 - The optical depth at which the wing become important is called the ***damping optical depth*** τ_{damp} .

$$W = \frac{b}{c} \int_{-\infty}^{\infty} du \left[1 - \exp \left(-\tau_0 e^{-u^2} \right) \right]$$

- The absorption line shape is almost “box-shaped.” The term in square brackets equals “1” until a certain value u_* and then, suddenly drops to “0”.
- We will define u_* to be the location at half maximum of the opacity function:

$$\exp \left(-\tau_0 e^{-u_*^2} \right) = \frac{1}{2} \longrightarrow u_*^2 = \ln (\tau_0 / \ln 2)$$

- Then, we have

$$W \approx \frac{b}{c} \int_{-u_*}^{u_*} du = \frac{b}{c} (2u_*) \longrightarrow W \approx \frac{2b}{c} \sqrt{\ln (\tau_0 / \ln 2)}$$

- Note that W is very insensitive to τ_0 (and thus N_ℓ) in this regime. Because W increases so slowly with increasing N_ℓ , this is referred to as the flat portion of the curve of growth.

-
- Inverting the above equation, we obtain

$$\tau_0 \approx (\ln 2) \exp \left[\left(\frac{cW}{2b} \right)^2 \right]$$

$$N_\ell \approx \frac{\ln 2}{\sqrt{\pi}} \frac{m_e c}{e^2} \frac{b}{f_{\ell u} \lambda_{\ell u}} \exp \left[\left(\frac{cW}{2b} \right)^2 \right]$$

$$N_\ell \approx 9.15 \times 10^{12} \text{ cm}^{-2} \left(\frac{0.4164}{f_{\ell u}} \right) \left(\frac{1215.67 \text{ \AA}}{\lambda_{\ell u}} \right) \left(\frac{b}{10 \text{ km s}^{-1}} \right)$$

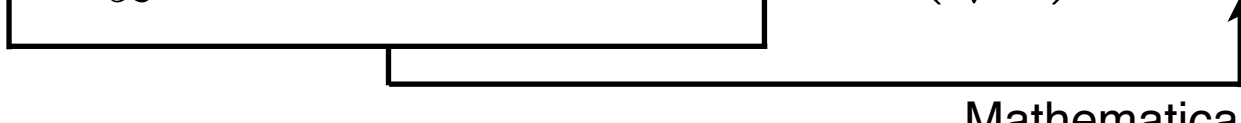
$$\times \exp \left[0.0152 \left(\frac{1215.67 \text{ \AA}}{\lambda_{\ell u}} \right)^2 \left(\frac{10 \text{ km s}^{-1}}{b} \right)^2 \left(\frac{W_\lambda}{0.01 \text{ \AA}} \right)^2 \right]$$

- The column density at a given equivalent width depends on the temperature, and thus on the thermal broadening.
- Any error in evaluating W_λ (from misestimating the continuum flux, for instance) will propagate exponentially into an error in N_ℓ .
- Therefore, it is advised not to use the above equation unless you have a very good idea of what the equivalent width W_λ and the thermal broadening b are for the line in question.

- **Damped Portion of the Curve of Growth, $\tau_0 \gtrsim \tau_{\text{damp}}$ (squar-root regime)**
- In this regime, the Doppler core of the line is totally saturated, but the “damping wing” of the Voigt profile start to contribute significantly to the equivalent width.

$$W = \frac{b}{c} \int_{-\infty}^{\infty} du \left[1 - \exp \left(-\tau_0 \frac{a}{\sqrt{\pi} u^2} \right) \right]$$

change of variables: Let $\tau_0 \frac{a}{\sqrt{\pi} u^2} = \frac{1}{x^2} \rightarrow u = \left(\frac{\tau_0 a}{\sqrt{\pi}} \right)^{1/2} x$

$$W = \frac{b}{c} \left(\frac{\tau_0 a}{\sqrt{\pi}} \right)^{1/2} \int_{-\infty}^{\infty} dx \left[1 - \exp(-1/x^2) \right] = \frac{b}{c} \left(\frac{\tau_0 a}{\sqrt{\pi}} \right)^{1/2} 2\sqrt{\pi}$$


Therefore, we have

$$W = \frac{b}{c} (4\sqrt{\pi} \tau_0 a)^{1/2} \quad a = \frac{\gamma_{\ell u}}{4\pi} \frac{1}{\nu_{\ell u}(b/c)} = \frac{\gamma_{\ell u}}{4\pi} \frac{\lambda_{\ell u}}{b}$$

$$W = \sqrt{\frac{b}{c} \frac{\tau_0}{\sqrt{\pi}} \frac{\gamma_{\ell u} \lambda_{\ell u}}{c}} \quad \longrightarrow \quad \tau_0 = \sqrt{\pi} \frac{c}{b} \frac{c}{\gamma_{\ell u} \lambda_{\ell u}} W^2$$

-
- In the book of Draine, he chooses the FWHM interval for the integration.

$$\exp\left(-\tau_0 \frac{a}{\sqrt{\pi} u_*^2}\right) = \frac{1}{2} \longrightarrow u_*^2 = \frac{\tau_0}{\sqrt{\pi}} \frac{a}{\ln 2}$$

$$W \approx \frac{b}{c} \int_{-u_*}^{u_*} du = \frac{b}{c} (2u_*) \longrightarrow W \approx \frac{2b}{c} \sqrt{\frac{\tau_0}{\sqrt{\pi}} \frac{a}{\ln 2}}$$

$a = \frac{\gamma_{\ell u}}{4\pi} \frac{1}{\nu_{\ell u}(b/c)} = \frac{\gamma_{\ell u}}{4\pi} \frac{\lambda_{\ell u}}{b}$

$$= \frac{1}{\sqrt{\pi \ln 2}} \sqrt{\frac{b}{c} \frac{\tau_0}{\sqrt{\pi}} \frac{\gamma_{\ell u} \lambda_{\ell u}}{c}}$$

- ▶ He note that this value is smaller than by a factor of $\sqrt{\pi \ln 2} = 1.476$. Multiplying by this factor, he obtain the same result as ours.
- ▶ This is equivalent to choosing the followings:

$$\exp\left(-\tau_0 \frac{a}{\sqrt{\pi} u_*^2}\right) = \exp\left(-\frac{1}{\pi}\right) = 0.7274$$

$$u_*^2 = \frac{\tau_0}{\sqrt{\pi}} (\pi a) = \pi \ln 2 \left(\frac{\tau_0}{\sqrt{\pi}} \frac{a}{\ln 2} \right)$$

$$N_\ell = \frac{m_e c^3}{e^2} \frac{1}{f_{\ell u} \gamma_{\ell u} \lambda_{\ell u}^2} W^2 = \frac{m_e c^3}{e^2} \frac{1}{f_{\ell u} \gamma_{\ell u} \lambda_{\ell u}^4} W_\lambda^2$$

$$N_\ell = 1.867 \times 10^{18} \text{ cm}^{-2} \left(\frac{0.4164}{f_{\ell u}} \right) \left(\frac{6.265 \times 10^8 \text{ s}^{-1}}{\gamma_{\ell u}} \right) \left(\frac{1215.67 \text{ \AA}}{\lambda_{\ell u}} \right)^4 \left(\frac{W_\lambda}{1 \text{ \AA}} \right)^2$$

- The equivalent width is proportional to the square-root of the optical depth. The column density (optical depth) is proportional to the square of the measured equivalent width.
- Furthermore, the column density is independent of the thermal broadening.
- The ***damping optical depth*** at which the transition from the flat to the damped portion of the curve of growth occurs are obtained by setting $W^{\text{flat}} = W^{\text{sq.-root}}$.

$$\frac{2b}{c} \sqrt{\ln(\tau_{\text{damp}} / \ln 2)} = \sqrt{\frac{b}{c} \frac{\tau_{\text{damp}}}{\sqrt{\pi}} \frac{\gamma_{\ell u} \lambda_{\ell u}}{c}}$$

$$\begin{aligned} \tau_{\text{damp}} &= 4\sqrt{\pi} \frac{b}{\gamma_{\ell u} \lambda_{\ell u}} \ln(\tau_{\text{damp}} / \ln 2) \\ &\approx 4\sqrt{\pi} \frac{b}{\gamma_{\ell u} \lambda_{\ell u}} \ln \left(\frac{4\sqrt{\pi}}{\ln 2} \frac{b}{\gamma_{\ell u} \lambda_{\ell u}} \right) \end{aligned}$$

Solution for $x = C \ln(x / \ln 2)$ with $C \gg 1$
 $x \approx C \ln(C / \ln 2)$

This solution is found to underestimate τ_{damp} by a factor of ~ 1.4 (~ 1.3) for $b = 1$ (10) km s^{-1} .

$$C \equiv 4\sqrt{\pi} \frac{b}{\gamma_{\ell u} \lambda_{\ell u}} = 93.1 \left(\frac{b}{1 \text{ km s}^{-1}} \right) \left(\frac{6.265 \times 10^8 \text{ s}^{-1}}{\gamma_{\ell u}} \right) \left(\frac{1215.67 \text{ \AA}}{\lambda_{\ell u}} \right)$$

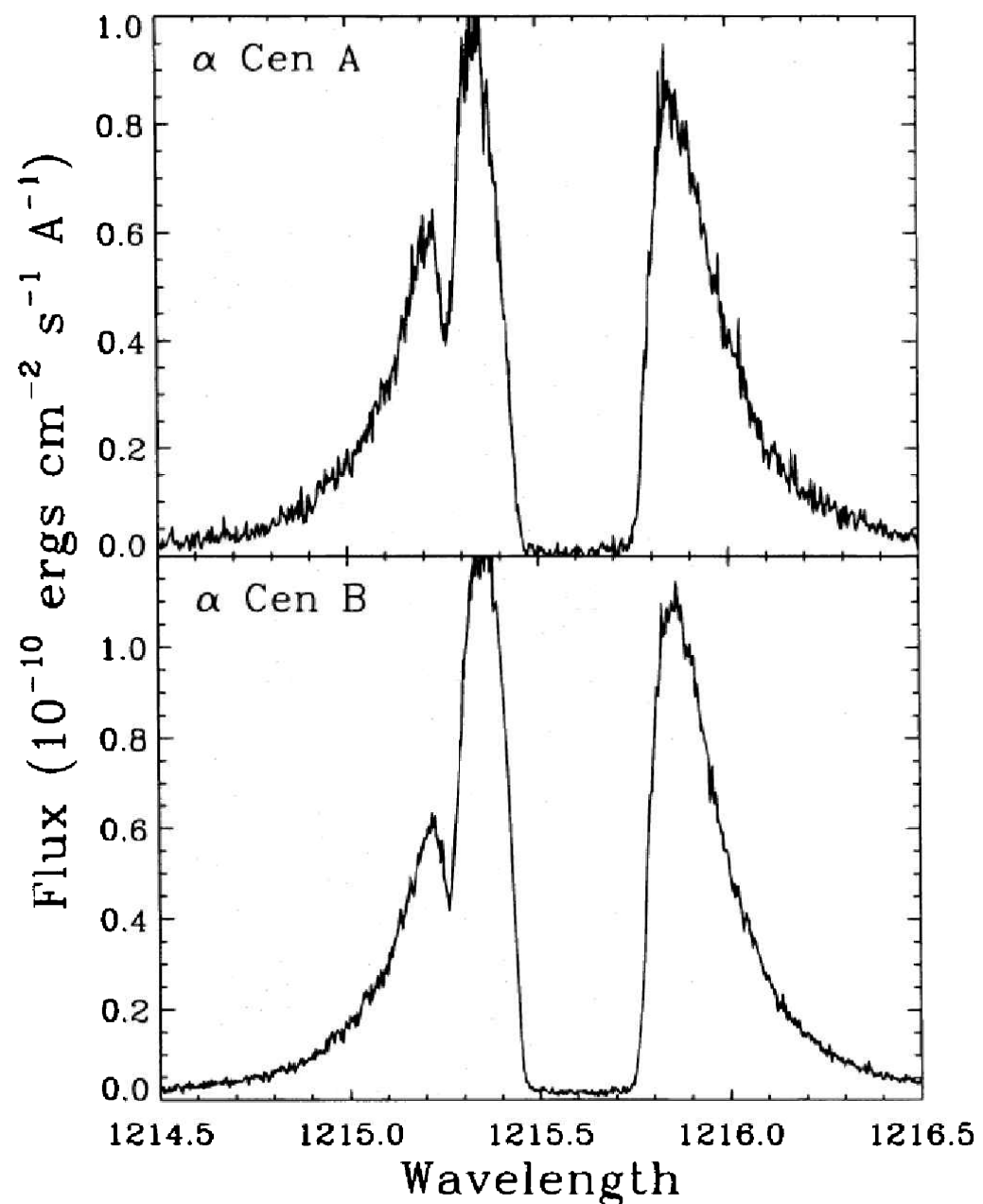
$$\begin{aligned} \tau_{\text{damp}} &\approx 93.1 \left(\frac{b}{1 \text{ km s}^{-1}} \right) \left(\frac{7616 \text{ cm s}^{-1}}{\gamma_{\ell u} \lambda_{\ell u}} \right) \ln \left[134 \left(\frac{b}{1 \text{ km s}^{-1}} \right) \left(\frac{7616 \text{ cm s}^{-1}}{\gamma_{\ell u} \lambda_{\ell u}} \right) \right] \\ &= 456 \left(\frac{b}{1 \text{ km s}^{-1}} \right) \ln \left[1 + 0.204 \ln \left(\frac{b}{1 \text{ km s}^{-1}} \right) \right] \\ &= 635 \left(\frac{b}{1.3 \text{ km s}^{-1}} \right) \ln \left[1 + 0.194 \ln \left(\frac{b}{1.3 \text{ km s}^{-1}} \right) \right] \\ &= 931 \left(\frac{b}{10 \text{ km s}^{-1}} \right) \ln \left[1 + 0.139 \ln \left(\frac{b}{10 \text{ km s}^{-1}} \right) \right] \end{aligned}$$

$$[N_{\ell}]_{\text{damp}} \approx \frac{4m_e c}{e^2} \frac{b^2}{f_{\ell u} \gamma_{\ell u} \lambda_{\ell u}^2} \ln \left[\frac{4\sqrt{\pi}}{\ln 2} \frac{b}{\gamma_{\ell u} \lambda_{\ell u}} \right]$$

$$[N_{\ell}]_{\text{damp}} = 1.23 \times 10^{16} [\text{cm}^{-2}] \left(\frac{0.4164}{f_{\ell u}} \right) \left(\frac{1215.67 \text{ \AA}}{\lambda_{\ell u}} \right) \left(\frac{b}{10 \text{ km s}^{-1}} \right) \left(\frac{\tau_{\text{damp}}}{931} \right)$$

Observations: H and D Ly α

- The study of Ly α absorption line is useful to studying the cold clouds in our galaxy. Ly α tends to be optically thick.
 - α Cen A and B ($d = 1.34$ pc) have broad Ly α “emission” lines from their hot chromospheres.
 - Superposed on the emission lines are optically thick absorption lines by the ISM.
 - For both α Cen A and B, $W_\lambda \approx 0.3$ Å.
- $\tau_0 = 68,000$, $b = 11.8 \text{ km s}^{-1}$ ($T = 8300 \text{ K}$)
- $N_\ell = 1.1 \times 10^{18} \text{ cm}^{-2}$
- This represents the regime where the flat part of the curve of growth gives way to the square-root part.
 - The stars are within our Local “Hot” Bubble so that the temperature is high. The column density imply that a density of 0.25 cm^{-3} .

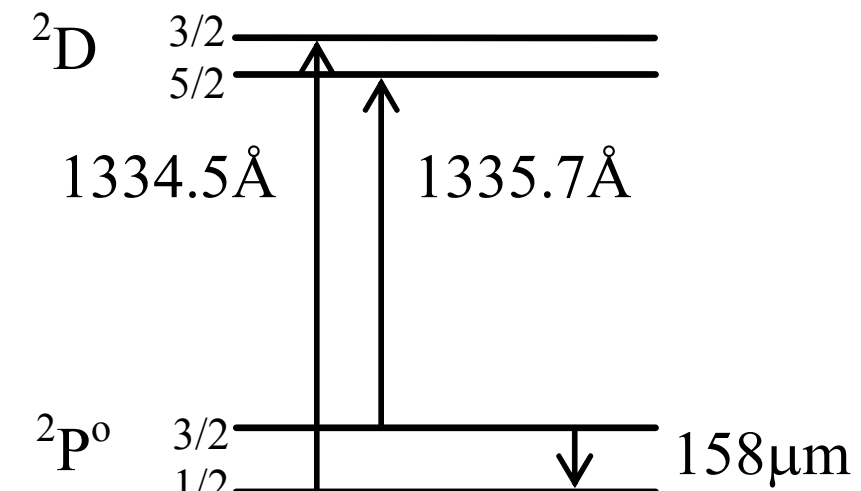


Ly α lines toward α Cen A (above) and α Cen B (below). Figure 2.8 in [Ryden], [Linsky & Wood 1996)

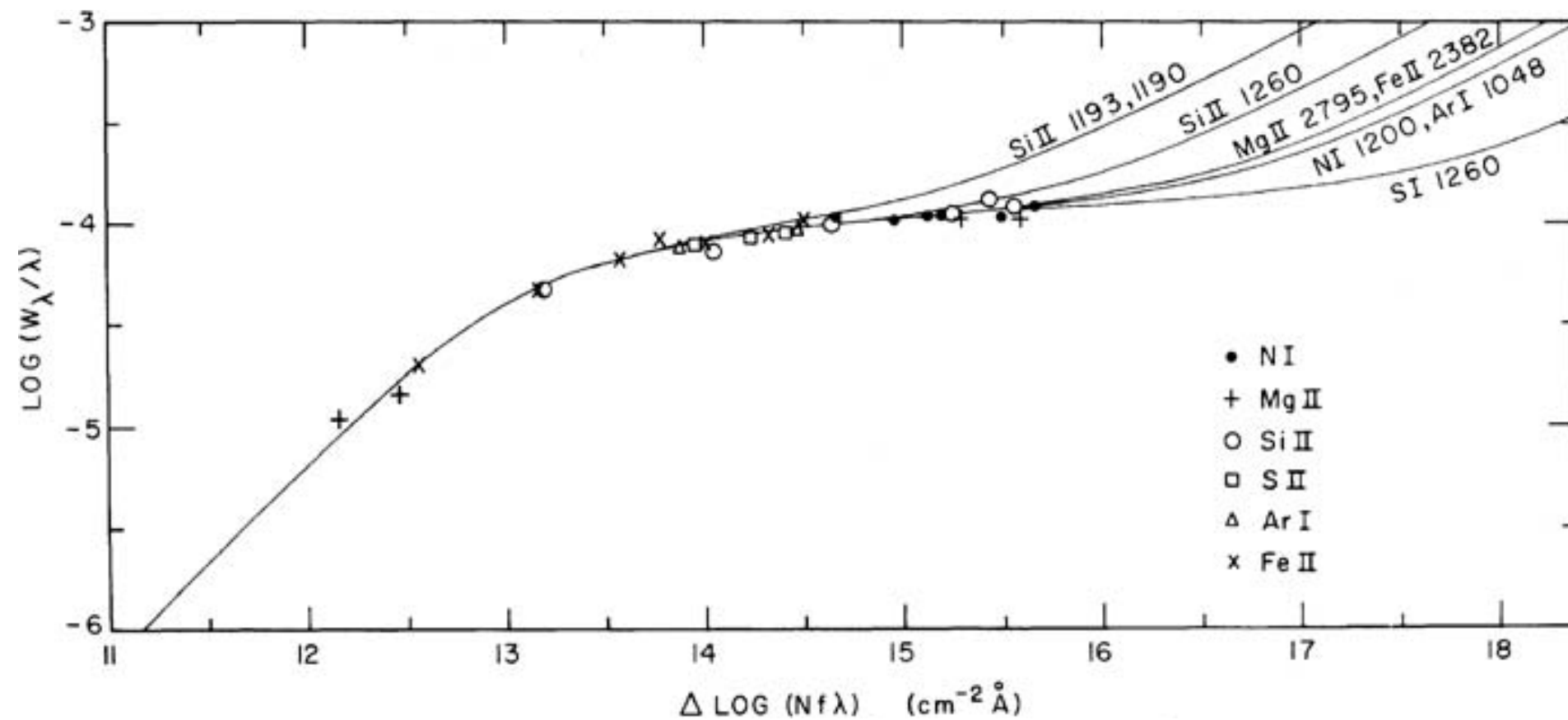
-
- On the left-hand slope of the Ly α emission lines, there is an optically thin absorption line. This is the absorption line of deuterium Ly α .
 - ▶ The deuterium Ly α lines are slightly blueshifted. wavelength for H Ly α = 1215.67Å, wavelength for deuterium Ly α is 1215.24Å.
 - ▶ The deuterium Ly α lines are optical thin, with $\tau_0 = 0.68$, and thus easier to interpret than the H Ly α from ordinary hydrogen. The column density of deuterium toward α Cen A and B, is $N_\ell = 6.1 \times 10^{12} \text{ cm}^{-2}$, giving a deuterium to hydrogen ratio $D/H \approx 6 \times 10^{-6}$. This is lower than the usual $D/H \approx 1.6 \times 10^{-5}$ in the Local Bubble, and is much less than the primordial value of $D/H \approx 2.5 \times 10^{-5}$.
 - For stars outside the Local Bubble, at $d \sim 100 \text{ pc}$, Ly α lines are in the square-root part of the curve of growth, with $W_\lambda \sim 10 \text{ Å}$, $N_\ell \sim 2 \times 10^{20} \text{ cm}^{-2}$, $n_\ell \sim 0.6 \text{ cm}^{-3}$.
 - We observe in the visible and UV spectrum of many stars a substantial number of atomic interstellar absorption lines.
 - The coexistence of Ca 0 and Ca $^+$ lines also allows us to obtain the degree of ionization of the corresponding cloud. We observe that Ca $^+$ is much more abundant than Ca 0 (ionization potential of Ca is 6.11 eV).

Observations: Absorption lines from fine-structure levels

- We also observe several absorption lines with wavelength close to each other, which comes from fine-structure levels of the fundamental ground state of the same atom or ion.
 - We can then directly obtain the relative populations of these levels. This gives valuable information on those physical parameters that determine their excitation, essentially the electron density.
 - For example, C II 1334.57Å and C II* 1335.70Å lines, which unfortunately are often saturated.
 - Morton (1975)'s observations of the C II and C II* ratio showed a significant population of atoms in $^2P_{3/2}^o$. This suggested that [C II] 157.7 μm line could be a strong cooling line in H I regions. It was not until the 1980s that the Kuiper Airborne Observatory detected Far-IR [C II] emission from the ISM, as predicted by Morton.
 - We may determine the cooling rate of the diffuse CNM due to [C II] 157.7 μm by observing the C II* 1335.70Å absorption line.
 - This observation gave a cooling rate of $\sim 3.5 \times 10^{-26} \text{ erg s}^{-1}$ per hydrogen nucleus (Pottasch et al. 1979; Gry et al. 1992), which is in agreement with the more direct determination of Bennett et al. (1994)



- Observed curve of growth for the ISM in front of the star ζ Oph (Morton 1975, ApJ)



- As can be seen in the above figure, most observed absorption lines lie on the Doppler plateau.
- Therefore, a better reduction technique than the use of curves of growth would be to adopt a fitting technique for the line profiles. This technique is the only one that can be used for complex line profiles.
- So, optical and UV absorption lines provide us useful information about the cold regions in the ISM. How much of each element and isotope is present? How hot is the gas? What are the integrated densities along the line of sight?

Observations: Abundances in H I Gas

- The gas phase abundances of many elements relative to H have been determined on many different sightlines using interstellar absorption lines.
- The observed gas-phase abundances vary from one sightline to another, which is presumed to reflect primarily variations in the amounts of various elements trapped in dust grains. Such removal of elements from the gas is known as ***interstellar depletion***.
 - Some elements, like Fe, are extremely under abundant in the gas phase, with gas-phase abundances that are typically only a few percent of the solar abundance.

| Element | Solar ^a | WIM $F_\star = -0.1$ | WNM $F_\star = 0.1$ | CNM $F_\star = 0.4$ | Diffuse H ₂ $F_\star = 0.8$ |
|--------------------|--------------------|-------------------------|------------------------|------------------------|---|
| C ^b | 295. | 114. | 111. | 109. | 93. |
| N | 74. | 62. | 62. | 62. | 62. |
| O | 537. | 592. | 534. | 457. | 372. |
| Na | 2.04 | (2.) | (2.) | (2.) | (2.) |
| Mg | 43.7 | 28.1 | 17.8 | 8.9 | 3.6 |
| Al | 2.95 | (0.54) | (0.27) | (0.097) | (0.025) |
| Si | 35.5 | 31.6 | 18.7 | 8.5 | 3.0 |
| S | 14.5 | 14.5 | 14.5 | 11.8 | 5.3 |
| Ca | 2.14 | (0.39) | (0.20) | (0.070) | (0.018) |
| Ti | 0.089 | 0.013 | 0.0052 | 0.0013 | 0.0002 |
| Fe | 34.7 | 5.2 | 2.9 | 1.19 | 0.36 |
| Ni | 1.74 | 0.32 | 0.16 | 0.057 | 0.015 |
| M^+ ^c | 432. | 197. | 168. | 142. | 107. |

^a From Table 1.4.

^b Gas-phase C abundance from Jenkins (2009) reduced by factor 2 (see text).

^c Photoionizable “metals”: $M = C + Na + Mg + Si + S + Fe + 3.9 \times Ni$.

Table 9.5 in [Draine], Jenkins (2009)

Gas-phase abundance vs. Condensation Temperature

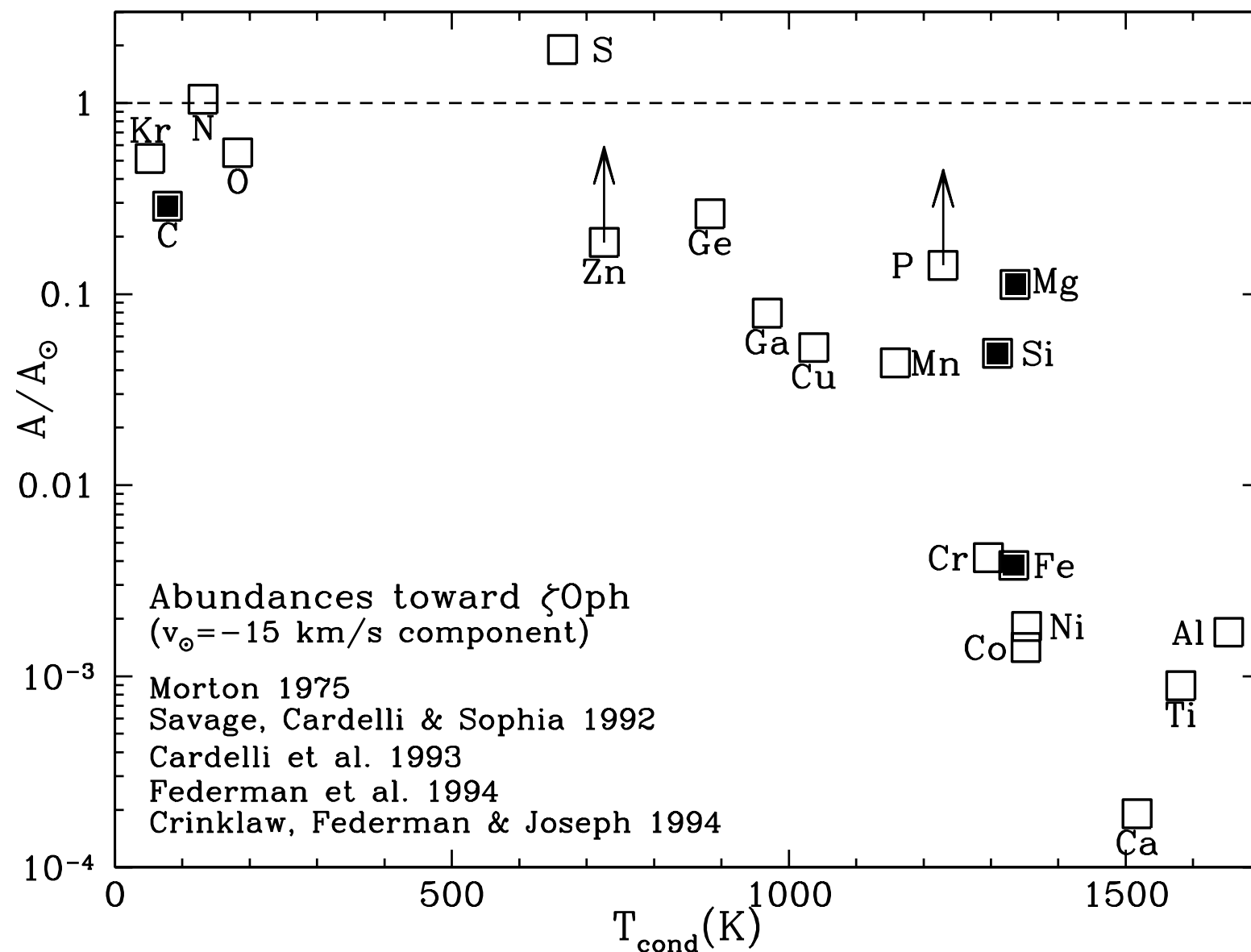


Figure 23.1 in [Draine]

Gas-phase abundances (relative to solar) in the diffuse cloud toward ζ Ophiuchi (O9.5V star, 138 pc), plotted versus “condensation temperature”. Solid symbols: major grain constituents C, Mg, Si, Fe. The apparent overabundance of S may be due to observational error, but may arise because of S II absorption in the H II region around ζ Oph. There’s a strong tendency for elements with high T_{cond} to be under abundant in the gas phase, presumably because most of the atoms are in solid grains.

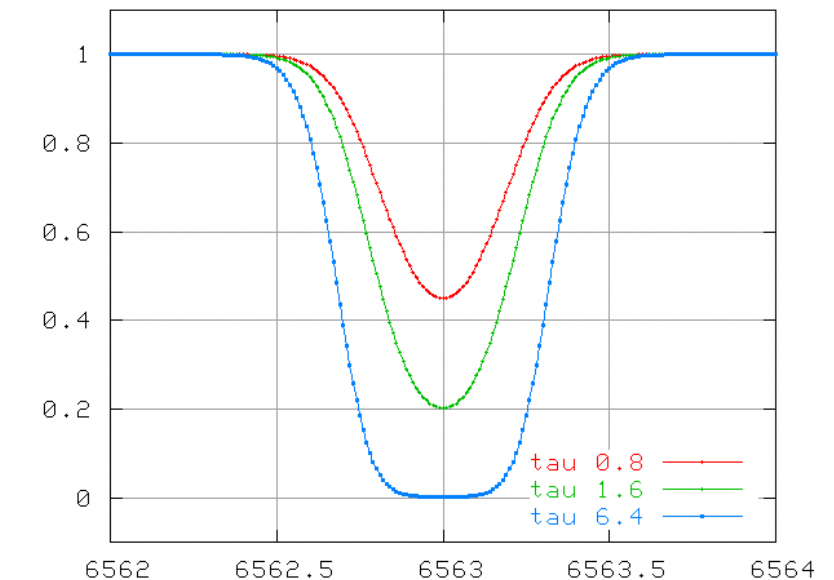
Condensation temperature : temperature at which 50% of the element in question would be incorporated into solid material in a gas of solar abundances, at LTE at a pressure $p = 10^2$ dyn cm $^{-2}$ (Lodders 2003).

Ly α Absorption System

- A structure along the line of sight to the quasar can be described by its neutral Hydrogen column density $N(\text{H I})$, the product of the density of the material and the path length along the line of sight through the gas.
- Historical classification

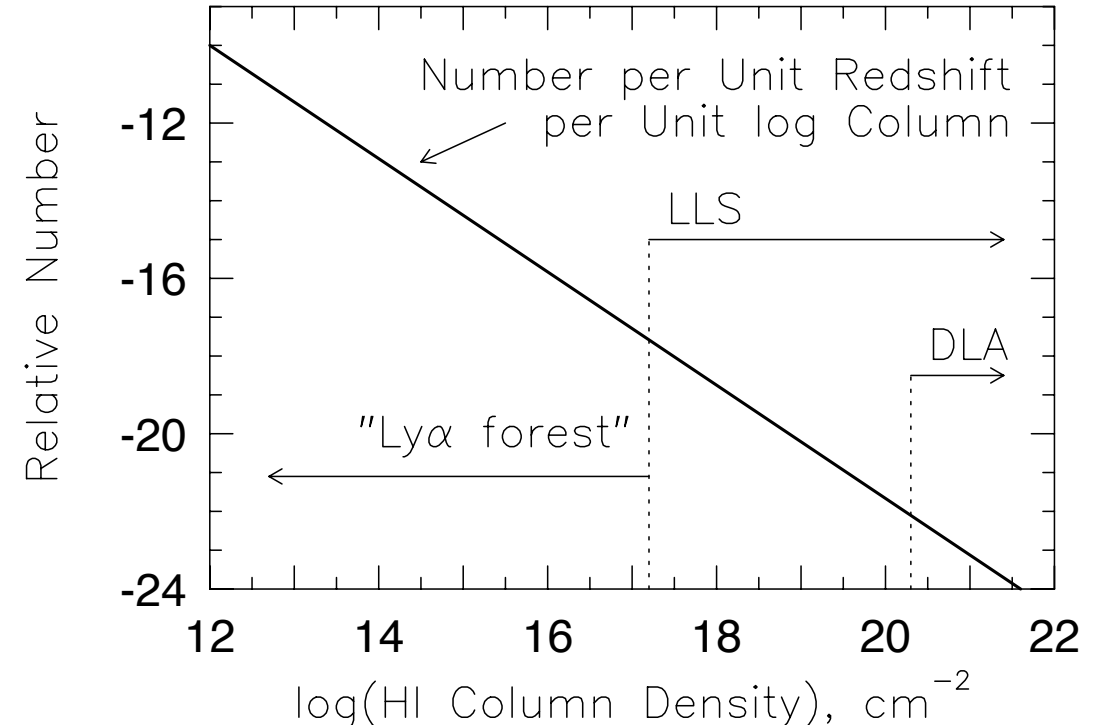
$$N(\text{HI}) = n_H L$$

| | |
|---|----------------------------|
| $N(\text{H I}) < 10^{12} \text{ cm}^{-2}$ | Currently not observable |
| $10^{12} < N(\text{H I}) < 10^{17.2} \text{ cm}^{-2}$ | Ly α forest |
| $10^{17.2} < N(\text{H I}) < 10^{20.3} \text{ cm}^{-2}$ | Lyman limit systems |
| $10^{20.3} < N(\text{H I})$ | Damped Ly α systems |



As $N(\text{HI})$ increases, the absorption line depth and width increase.

- Column density distribution
 - There are many more weak lines than strong lines.
 - The column density distribution roughly follows a power-law.



Homework - Transition from Doppler core to Lorentzian wing

- Use the Newton-Raphson method

- The numerical solution for $f(x) = 0$ can be found iteratively: $x_{n+1} = x_n - \frac{f(x_n)}{f'(x_n)}$

(1) Apply the interactive equation to our problem by defining a function:

$$f(x) = x - \ln(\sqrt{\pi}/a) - \ln x \quad (x \equiv u^2)$$

Show that the iterative solution can be expressed: $x_{n+1} = \frac{\ln(\sqrt{\pi}/a) - 1 + \ln x_n}{1 - 1/x_n}$

(2) Find a numerical solution $x = x_*$ for Ly α and $b = v_{\text{th}} = 10 \text{ km s}^{-1}$.

You may choose an initial guess to be, for instance, $x_0 = 10$ for a root of $f(x) = 0$.

(3) Let's denote the width parameter as a_* for this solution x_* , meaning that

$$x_* - \ln(\sqrt{\pi}/a_*) - \ln x_* = 0$$

Now, for any parameter a which is different from a_* , you may express the constant term in $f(x)$ as follows:

$$\ln(\sqrt{\pi}/a) = \ln(a_*/a) + \ln(\sqrt{\pi}/a_*)$$

To find the solution for $a \neq a_*$ (but, $a \approx a_*$), choose an initial guess to be $x_0 = x_*$. Show that the solution for this a is given by (after only a single iteration)

$$\begin{aligned}x_1 &= x_* + \frac{x_*}{x_* - 1} \ln(a_*/a) \\&\approx x_* + \ln(a_*/a) \quad \text{if } x_* \gg 1\end{aligned}$$

- (4) Show that the above equation is the same as our solution shown in this lecture note and also Eq. (6.42) in Draine's book.
- (5) We note that Eq. (2.32) in Ryden's book (our textbook) is wrong. Derive a correct solution for $b = 1.3 \text{ km s}^{-1}$, which is appropriate for Ly α in the CNM with $T \sim 100 \text{ K}$.